Part V

JET FORMATION AND DYNAMICS

Relativistic Jet Formation in Microquasars

David L. Meier
Jet Propulsion Laboratory, California Institute of Technology

Abstract. Microquasars produce collimated, relativistic flow at speeds up to a Lorentz factor of ~ 3 (0.94c). It is generally believed that such flow velocities indicate that jet acceleration and collimation occurs in the relativistic environment of a supermassive black hole. Recently, several groups around the world have begun to test theories of jet formation using magnetohydrodynamic (MHD) simulations of magnetized gas flow around black holes. This paper reviews the field of simulations of MHD jet formation, with an emphasis on producing the observed jet speeds and on the role that black hole angular momentum might play. It is shown that the most powerful jets occur when the black hole is rotating rapidly *and* when the accretion disk is geometrically thick and hot. This model may explain the association of jet ejection with the hard state in microquasars.

Keywords: accretion, accretion disk, black hole physics, jet, magnetohydrodynamics, X-ray:stars

1. Introduction

The distinguishing feature that separates microquasars from other binary X-ray sources, and links them with the giant extragalactic radio galaxies and quasars, is the presence of twin relativistic jets emanating from the source center. Two important observations indicate that the jets are ejected from deep within the potential well of the accreting compact object and, therefore, are closely related to the accretion process itself. First of all, the speed of the jet is of order the escape velocity from the vicinity of the compact object — 0.26 c for SS433 (Margon, 1984), which is believed to harbor a neutron star, and 0.92 c (Lorentz factor $\Gamma = (1-v^2/c^2)^{-1/2} \approx 2.5$) for GRS 1915+105 and GRO J1655-40 (Mirabel & Rodriguez, 1999), which are believed to contain black holes of several solar masses. Secondly, jet ejection does not take place unless the accretion disk has entered a hard X-ray state (Fender *et al.*, 1999), and then the actual ejection event often is accompanied by a temporary disappearance of the hard X-ray emission, a possible indication that the hot disk material has been ejected in the jet.

The leading model for producing and collimating relativistic jets is the magnetohydrodynamic (MHD) acceleration model (Lovelace, 1976; Blandford, 1976). This model is able to account for jet collimation, acceleration to relativistic velocities, and the magnetic fields associated with detected synchrotron emission, all while operating within the accretion paradigm for microquasars. In addition, recent results have shown that it can account for the observed association of jet production with the black hole accretion disk states (Meier, 2001b).

This paper reviews some of the important properties of numerical simulations of MHD jet acceleration and discusses analytic work that combines theories of accretion disk structure, disk dynamos, and jet production to explain microquasar behavior.

2. Review of Numerical Simulations of Jet Production by Magnetized Accretion Disks

Recent results on numerical simulations of jet production by magnetized accretion disks also have been reviewed by Meier & Koide (2000), Meier (2001a), and Meier, Koide, & Uchida (2001). The simulations fall into two general categories: a) time-dependent, useful for studying violent and transient effects, and b) steady-state, useful for studying more benign, longer-lived phenomena.

2.0. Non-relativistic Time-dependent Simulations: The Basic Acceleration and Collimation Mechanism

The basic mechanism for acceleration and collimation of jets by rotating magnetic fields was described in detail by Blandford & Payne (1982) for accretion disks and Blandford & Znajek (1977) for rotating black holes. The first authors to demonstrate this mechanism with numerical simulations were Uchida & Shibata (1985). Some of the best modern illustrations of their "sweeping pinch" mechanism are the three-dimensional renderings of the 2.5-dimensional simulations of Uchida *et al.* (2000). These simulations begin with a *strong* vertical magnetic field threading a differentially-rotating, thick accretion torus. The differential rotation winds up the field into a toroidal component (B_ϕ). The vertical magnetic pressure gradient ($\partial B_\phi^2/\partial Z$) quickly becomes strong enough to accelerate the disk surface layers upward, and the radial hoop stress ($-B_\phi^2/R$) pinches and collimates the outflow into a jet, with and outflow speed of order the escape velocity from the inner edge of the disk or torus. Such an outburst is a very dynamical event, occurring in only a few tens of milliseconds for a $10\,M_\odot$ black hole disk; a violent microquasar outburst lasting hours or days might involve many such events strung together in rapid-fire fashion.

2.0. Non-relativistic Steady-State Simulations

In low-luminosity, quiescent sources, the accretion and jet ejection process may reach a steady or quasi-steady state. Recently many papers have studied steady jet ejection numerically (e.g., Ustyugoga *et al.*, 1995; Ouyed & Pudritz, 1997; Krasnopolsky *et al.*, 1999). In these calculations the thick disk is replaced by an infinitely-thin disk boundary condition on the equatorial plane, with a poloidal (R, Z) magnetic field anchored in the differentially-rotating disk and matter injected from the lower boundary along the field lines at a speed slower than the escape speed. While the axial field and velocity (B_Z and V_Z) and azimuthal velocity (V_ϕ) are fixed on the lower boundary, the radial components (B_R and V_R) and azimuthal field are allowed to change as the solution is obtained. The final numerical results are indeed very similar to those of Blandford & Payne (1982). The field lines must have a polar angle of $\theta > 30\,\mathrm{deg}$ in order for magnetically-driven outflow to commence, but well above the disk the field lines bend toward the axis, resulting in a slowly-collimated wind or jet, again with a terminal velocity of order the escape speed at the foot of the jet. Such a scenario appears to be a good model for the steady compact radio cores seen continuously in sources like Cyg X-1 and GX 339-4, or in GRS 1915+105 between outbursts (Dhawan *et al.*, 2000).

2.0. Pseudo-Relativistic Simulations of Black Hole Accretion Systems

To study the dynamical strong field problem in very tenuous coronae, the author and his colleagues have employed non-relativistic simulations, also with an infinitely thin disk boundary condition, and interpreted them in a pseudo-relativistic manner (Lind *et al.*, 1994; Meier *et al.*, 1997). That is, as long as the inertia of the magnetic field and internal energy are small ($c_{sound} < c$; $V_A < c$), the non-relativistic MHD equations have the same form as the relativistic ones if the velocity V is replaced with the proper velocity $U \equiv \Gamma V$. When U exceeds c (unity here), it can be identified with the Lorentz factor Γ. Thus, these pseudo-relativistic simulations account for the inertia of the kinetic energy, which will be important even for a cold gas.

The initial conditions for these simulations are very similar to those of the steady-state ones, except that the disk is truncated interior to the last stable orbit, and B_R, V_R, and B_ϕ are all *fixed* on the lower boundary, as would be the case in an actual accretion disk. These conditions result in a new magnetic field structure during the simulation: the anchored field lines at the inner edge of the disk are bent inward, creating a substantial B_R in the corona, which is then wound

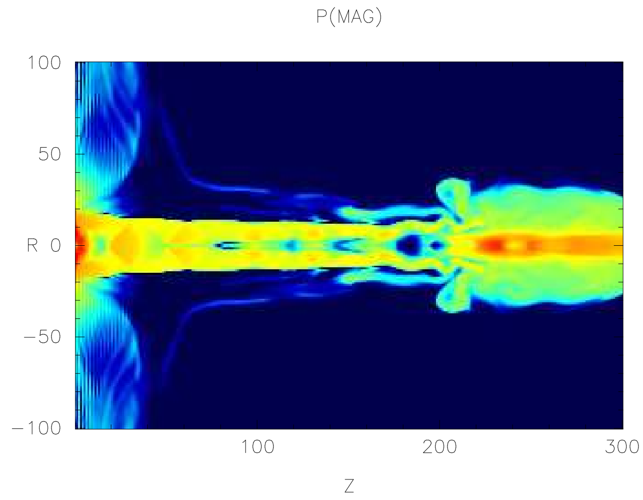

Figure 1. Magnetic pressure intensity plot at time $t = 700\tau_g$ for a simulated jet produced by a Keplerian accretion disk (on the equator at left) around a black hole (at [0,0]). Red indicates the highest magnetic pressure and dark blue the lowest. Such a plot is similar to the appearance of a total intensity radio image (if the field/particle ratio is uniform). Distances are in units of r_g.

up by the differential rotation into B_ϕ, expelling plasma upward and pinching it into a collimated jet. The simulation at late times is shown in Figure 1 and details of the magnetic structure near the disk inner edge are shown in Figure 2. This highly-collimated inner jet appears to compete with the outer, loosely-collimated wind found in the steady state simulations: in the ~ 80 simulations we have run, we see either the inner jet or wind, but rarely both at the same time.

The pseudo-relativistic simulations have been useful for studying a possible mechanism for producing the highly relativistic jets ($\Gamma \gtrsim 10$) observed in radio galaxies and quasars — the "magnetic switch" — which achieves jet velocities higher than the escape speed by accelerating a very tenuous disk corona rather than the dense disk material. However, as the speeds of the fastest microquasar jets agree well with the escape velocity from the ergosphere of a rotating black hole, it appears unnecessary at this time to invoke such a mechanism for microquasars. On the other hand, the discovery of objects with high Lorentz factors ("microblazars") could change this situation.

2.0. Fully General Relativistic Jet Production Near Rotating Black Holes

The full jet acceleration problem involves MHD processes in curved spacetime near the black hole horizon. Our fully relativistic simulations

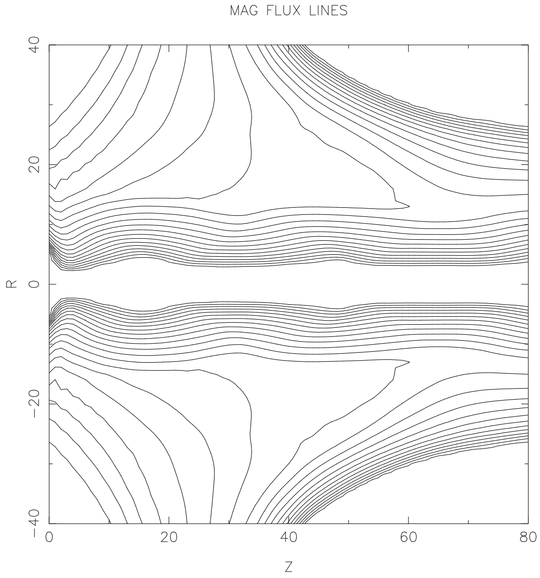

Figure 2. Field structure of the inner disk edge for the simulation in Figure 1. The black hole is at the origin and the expanded scale is again in r_g.

begin with a rather thick accretion disk, with inner edge at $R = 6\,r_g$, threaded by a weak axial magnetic field (internal Alfven velocity of $V_A = 0.01c$). In addition to the disk, a freely-falling halo fills the remainder of the computational grid, which extends from $1.5\,r_g$ to $40\,r_g$ in spherical radius and from 0 to $\pi/2$ in polar angle. Five different scenarios have been simulated in a series of papers involving different combinations of rotating ($j \equiv J/(GM^2/c) = 0.95$) and non-rotating holes and rotating, non-rotating, and counter-rotating disks. The simulations were followed for a fairly short period of time — on the order of $\sim 100\tau_g \equiv 100\,GM/c^3$ — but long enough to allow the rotation of the disk or geometry and MHD processes to run their course.

The Schwarzschild cases had no significant MHD-driven outflow develop unless the disk was rotating. The outflow velocity was of order the escape velocity from the last stable orbit of $6r_g$ ($0.4c$) (Koide *et al.*, 1999). In the Kerr cases, however (Koide *et al.*, 2000), a powerful jet resulted *even when the disk was not rotating or was counter-rotating against the black hole.* The main driver of the jet was the rotating geometry itself, rather than the rotation of the accretion disk. The disk fell rapidly into the ergospheric region ($R < 2r_g$), where the accreting matter must rotate with the black hole geometry. This rotation drove an MHD jet in a manner similar to the non-relativistic rotating disk simulations. The highest jet speeds achieved so far in these simulations are of order the escape velocity from the edge of the ergosphere ($\Gamma < 3$).

3. Applications to Microquasars

3.0. Jet Power

One of the most important properties of jets is the total amount of energy per unit time carried away from the central engine by the jet. It is shown in Meier (2001b) that the jet power from a rotating, magnetized accretion flow can be computed from the following expression

$$L_{jet} \;=\; B_\phi^2\, H^2\, R^2\, \Omega^2 \,/\, 4\, c \tag{1}$$

where B_ϕ is the strength of the azimuthal magnetic field responsible for much of the viscous stress, H the disk scale height, R the radius of the jet-emitting region, and Ω the angular velocity of the magnetic field as measured by an observer at infinity. Ω actually is composed of two parts: rotation of the metric space surrounding the (possibly-spinning) black hole and rotation of the accretion disk within that metric

$$\Omega \;=\; \Omega_m \;+\; \Omega_d \tag{2}$$

The factor $B_\phi H$ represents the poloidal magnetic field strength protruding from the disk surface — only a fraction of the toroidal component — as suggested by dynamo theory arguments (Livio *et al.*, 1999; Vishniac, private communication) and simulations (Khanna, 1999). With a given accretion model, the jet power can be computed from (1).

3.0. Specific Examples

3.0.0. *Poor jet-producing quality of thin, cool accretion disks*

We first consider standard, Shakura & Sunyaev (1973) disks around Kerr and Schwarzschild black holes. (For more details see Meier, 2001b.) With $\Omega = \Omega_d = \Omega_{K(epler)}$ at $R \approx 7GM/c^2$ in the Schwarzschild case, and $\Omega = \Omega_m + \Omega_K$ at $R \approx 2GM/c^2$ in the Kerr case

$$L_{jet}^{Sch-SS} \;=\; 10^{35.4}\,\mathrm{erg\,s^{-1}}\, m_1^{0.9}\, \dot{m}_{-1}^{1.2} \tag{3}$$

$$L_{jet}^{Kerr-SS} \;=\; 10^{36.3}\,\mathrm{erg\,s^{-1}}\, m_1^{0.9}\, \dot{m}_{-1}^{1.2}\,(1 + 1.1j + 0.29j^2) \tag{4}$$

where m_1 is the black hole mass in $10M_\odot$ units, $\dot{m}_{-1}$ is the accretion rate in units of the Eddington rate of $2.2 \times 10^{-7}\, M_\odot\, yr^{-1} m_1$. The jet powers in equations (3) and (4) are weaker by orders of magnitude than those observed in sources like GRS 1915+105 and others ($10^{39-40}\,\mathrm{erg\,s^{-1}}$). The chief reason for the predicted jet powers being so small is the weak poloidal magnetic field, due to the cool, geometrically thin ($H << R$) nature of the disks.

As several authors have pointed out, black hole spin in the thin disk case makes little difference in the jet power, regardless of whether one is comparing non-rotating systems with rotating ones ($10^{35.4}$ *vs.* $10^{36.4}\,\mathrm{erg\,s^{-1}}$) or the contribution of disk power *vs.* hole power within the same system ($10^{36.5}$ *vs.* $10^{36.2}\,\mathrm{erg\,s^{-1}}$). The most noticeable effect of hole rotation in these cases is that the jet is produced at a smaller radius, resulting in somewhat larger field strengths and rotation rates.

3.0.0. *Importance of black hole spin and hot, thick accretion flows*
The situation is quite different when the disk is hot and geometrically thick: $B_p \sim B_\phi$ should produce much stronger jets. However, thick disks generally rotate more slowly than the Keplerian rate, so the jet power still should be rather small, *unless the metric rotates as well.*

At the present time the theory of hot, geometrically thick accretion flow is in a state of flux; new models (CDAFs, Narayan *et al.*, 2000; and ADIOSs, Begelman & Blandford, 1999) are being proposed to replace the standard advection-dominated ones (Narayan & Yi, 1995). Because the ADAFs are the most developed, they are used here to illustrate the main points, but the computations should be re-done when the theory of hot accretion flows has stabilized. Inserting ADAF solutions for $H(\sim R)$, B_ϕ, and $\Omega_d \approx \Omega_K$ into equation (1) we obtain

$$L_{jet}^{Sch-AD} = 10^{36.5}\,\mathrm{erg\,s^{-1}}\,m_1\,\dot{m}_{-1}\,f^2 \tag{5}$$

$$L_{jet}^{Kerr-AD} = 10^{38.0}\,\mathrm{erg\,s^{-1}}\,m_1\,\dot{m}_{-1}\,(0.5f^2+1.5fj+1.0j^2)\,g^2 \tag{6}$$

where $f = \Omega_d/0.4\Omega_K$ (possibly much less than unity) and $g = B_\phi/B_\phi^{AD}$ (possible greater than unity because of shear in the metric not yet taken into account). In the hot Kerr case, most of the jet power is derived from the rotational energy of the black hole, not from the released binding energy of the presently-accreting matter. (The implicit dependence on $\dot{m}$ enters through the disk magnetic field strength.) The situation for hot, thick flows, therefore, is quite different from that for cool geometrically thick accretion flows. The poloidal field is much stronger, and, when the black hole also rotates, very strong jets are produced.

4. Discussion and Conclusions

The above model explains a number of features of microquasars:

- Jet powers up to $10^{39-40}\,\mathrm{erg\,s^{-1}}$ for a $10\,M_\odot$ black hole
- A suppression factor of $63\,m_1^{0.1}\,\dot{m}_{-1}^{-0.2}\,g^2$ in the jet power when the accretion transitions from a hard to a soft state (which compares well with the > 35 factor observed)

– Jet speeds of order $\Gamma_{escape} = \alpha_{lapse}^{-1} = \{[1+(1+2r_g/r)(jr_g/r)^2]/[1-2r_g/r + (jr_g/r)^2]\}^{1/2} \approx 2.4$ if the jet is ejected from the ergosphere ($r = 2r_g$) of a Kerr hole at the local escape speed.

Chief among the things the model cannot explain is why GRO J1655-40 began as a radio loud microquasar but evolved to a radio quiet one, despite repeated accretion events that appear very similar to the one that triggered the initial jet (Tavani *et al.*, 1996).

Acknowledgements

Part of this research was carried out at the Jet Propulsion Laboratory, California Institute of Technology, under contract to NASA.

References

Begelman, M. C. & Blandford, R.D. *M.N.R.A.S.*, 303, L1–5, 1999.
Blandford, R.D. *M.N.R.A.S.*, 176, 465–81, 1976.
Blandford, R. D. & Znajek, R. *M.N.R.A.S.*, 179, 433, 1977.
Blandford, R. D. & Payne, D. G. *M.N.R.A.S.*, 199, 883, 1982.
Dhawan, V., Mirabel, I.F., & Rodriguez, L.F. Available as astro-ph/0007086.
Fender, R. *et al.*. *Astroph. J.*, 519, L165–8, 1999.
Khanna, R. In A. F. Moz & M. Nunez, ed., ASP Conf. Series, Vol. 178, p. 57, 1999.
Koide, S., Shibata, K., & Kudoh. *Astroph. J.*, 522, 727, 1999.
Koide, S., Meier, D., Shibata, K., & Kudoh. *Astroph. J.*, 536, 668, 2000.
Krasnopolsky, R., Li, Z-Y, & Blandford, R. *Astroph. J.*, 526, 631–42, 1999.
Lind, K., Meier, D., & Payne, D. *B.A.A.S.*, 184, 1994.
Livio, M. Ogilvie, G. I., & Pringle, J. E. *Astroph. J.*, 512, 100, 1999.
Lovelace, R.V.E. *Nature*, 262, 649–52, 1976.
Margon, B. *Ann. Rev. Astron. Astrophys.*, 22, 507–36, 1984.
Meier, D. L. In R. Laing & K. Blundell, ed. *Particles and Fields in Radio Galaxies*, proceedings of an Oxford workshop, Oxford, U.K., August, 2000. ASP Press.
Meier, D. *Astroph. J. Letters*, in press, 2001.
Meier, D. L. & Koide, S. In H. Hirabayashi, P.G. Edwards, & D. W. Murphy, ed. *Proceedings of the First VSOP Symposium*, Sagamihara, Japan, January 2000.
Meier, D. L. Koide, S., & Uchida, Y. *Science*, in press, 2001.
Meier, D. *et al.*. *Nature*, 388, 350, 1997.
Narayan, R. & Yi, I. *Astroph. J.*, 444, 231, 1995.
Narayan, R., *et al.* *Astroph. J.*, 539, 793–808, 2000.
Ouyed, R. & Pudritz, R. *Astroph. J.*, 482, 712, 1997.
Mirabel, I. F. & Rodriguez, L. F. *Ann. Rev. Astron. Astrophys.*, 37, 409–43, 1999.
Shakura, N. I. & Sunyaev, R. A. *Astron. Astroph.*, 24, 337–355, 1973.
Tavani, M. *et al.*. *Astroph. J.*, 473, L103–6, 1996.
Uchida, Y. & Shibata, K. *Publ. Astron. Soc. Japan*, 37, 515, 1985.
Uchida, Y. *et al.*. In Martens, P.C.H., Tsuruta, S., & Weber, M.A., ed., ASP Conf. Series, Vol. 195, p. 213, 2000.
Ustyugova, G. *et al.*. *Astroph. J.*, 439, L39–8, 1999.

The Continuous Jets of Cygnus X-1

R. Spencer, C. de la Force
Jodrell Bank Observatory, University of Manchester

A. Stirling, M. Garrett, R. Fender, R. Ogley
University of Central Lancashire, UK; JIVE, The Netherlands; University of Amsterdam; SACLAY, Paris

Abstract. A resolved jet-like radio-emitting structure on mas scales has been found in Cygnus X-1. The jet emission is relatively smooth, and does not show the knots and blobs seen in Cygnus X-3, SS433 and GRS1915+105. This suggests that the jet production mechanism in Cyg X-1 is continuous, with the steady production of the energetic electrons and magnetic field required for the production of the radio emission. This is unlike the episodic jets seen in the other sources. The implications of these results for jet formation mechanisms will be discussed.

Keywords: X-ray binary, jet, Cyg X-1

1. Introduction

Cygnus X-1 (V1357 Cygni) was one of the earliest stars to be detected in the radio band (Braes and Miley 1971; Hjellming and Wade 1971). Its radio flux density has occasionally reached levels of 50 mJy in the 1970's, however it is mostly at the 12–15 mJy level with a flat ($\alpha = 0$) spectrum to mm wave frequencies (Fender et al. 2000a). The source also has long periods in the low/hard state (Brocksopp et al. 1999), with transitions to the soft state being associated with changes in the radio emission. It is one of the best candidates for a black hole compact companion. However its radio structure has remained a mystery until recent VLBI observations.

About a dozen of the radio emitting X-ray binary stars have been found to possess radio jets. Some sources show superluminal motion (e.g. GRS 1915+105; Fender et al. 1999), others have lower but still relativistic velocities (e.g. SS433, Paragi et al. this conference). They typically have very 'blobby' structures where the ejection of knots of emission can in some cases be related to changes in X-ray state (see review by Mirabel and Rodriguez, 1999). The flat spectrum and steady radio emission in the low/hard state of Cyg X-1 suggests that its radio properties may be somewhat different from these sporadic and transient sources.

Cyg X-1 is used as part of the astrometric reference frame, and the hint of resolution effects in trans-Atlantic VLBI measurements by

Lestrade (priv. comm.) led us to propose VLBA observations on this source.

2. VLBA Observations

Initial observations were undertaken in March 1997 at 15 GHz. These showed the presence of a jet-like structure on the ~ 1 mas scale (Stirling et al. 1998). More comprehensive follow-up observations were made in August 1998, over three epochs (10, 12 and 14 August) and at two frequencies (8.4 and 15 GHz). The results found previously at 15 GHz were confirmed, though the possible existence of emission in a direction perpendicular to the jet , again on the 1 mas scale, cannot be ruled out.

The 8.4 GHz observations however show a clear one-sided jet ~ 15 mas (30 au if at 2 kpc) at position angle ~ -20 degrees present at each epoch. The emission along the jet varies smoothly, and is unlike the blobby jets seen in GRS1915+105 and SS433 (Stirling et al. 2000). However it should be noted that a compact jets exist in GRS 1915+105 when in the 'plateau' state (Dhawan et al. 2000). The properties of steady jets produced by both persistent and transient sources in the low/hard state are discussed in Fender (2000b).

A kink in the jet (see image presented by de la Force et al., this conference) stays consistent between the epochs, indicating a slow ($<$ 3000 km s^{-1}) jet, a backward moving shock feature or precession with non-ballistic flow. The smooth emission suggests a continuous jet, as described by the models of Blandford and Königl (1979) and where the fading of brightness down the jet is caused by adiabatic expansion rather than energy losses of the radiating electrons.

3. Jet Energetics

The brightness ratio of the jet to the counter-jet region in the map exceeds 64 to 1. If we interpret this as being due to Doppler boosting of a relativistic jet then $\beta \times cos(\theta) = 0.6$ for a spectral index of 0. The inclination angle for the binary has been proposed to be at 37 degrees, so if the jet is at the same angle then $\beta = 0.78, \gamma = 1.59$, and $\beta_{app} = 1.25$. We would therefore expect to see an apparent motion of 110 mas/day of the components in the jet.

Assuming synchrotron radiation, a cylindrical jet, unity filling factor, and ignoring the contribution from protons, we find a minimum energy of 10^{39} ergs. If the time to form the jet is equal to the time for material to travel down the length of jet then the power in the 15 mas jet is $\sim 3 \times 10^{34}$ ergs/sec. This is rather less than the minimum power required for discrete blob ejection in GRS1915+105 (10^{39} ergs/sec). However if the flat spectrum extends to infra-red frequencies the power increases to 10^{37} ergs/sec for the whole jet, which is comparable to the bolometric X-ray luminosity in this state.

The power required for continuous jets in persistent sources may be much less than that for sporadic jets in transient sources. We might therefore expect less dramatic physical changes in persistent sources as a result, consistent with long periods in the low/hard state.

The inner core of the jet (as shown in the 15 GHz images) is $\sim 1 \times < 0.5$ mas^2 in size, or 2 au in length. The equipartition magnetic field B is then $\sim$ 300 mG, resulting in an electron lifetime, $t_{yr} = \frac{1}{(B^3 \nu_{GHz})^{0.5}}$, of 1.6 years at 15 GHz and 22 days at IR. These are very much greater than the travel times down the jet if the bulk motion is relativistic and show that the losses down the jet are primarily adiabatic. The typical energy of the electrons radiating at 15 GHz in this field is 100 Mev.

The expected magnetic field at the inner disk ($\sim 6r_g$) is 2×10^{11} G if $B \propto r^{-2}$ or 3×10^5 G if $B \propto r^{-1}$ as in the Hjellming and Johnston (1988) models. The jet power for the core region can be estimated from $L_j > \pi r^2 \Gamma^2 \beta c U_{min}$ where U_{min} is the minimum energy density. Ignoring the protons again gives 9×10^{34} ergs/sec for the inner jet, comparable with the figure found above for the jet as a whole.

Several mechanisms for the production of steady jets have been proposed. Ones which may be relevant here are the Blandford and Payne (1982) (BP) method which uses the twisting of magnetic fields generated in a disk to accelerate a jet, and the Blandford and Znajek (1977) (BZ) mechanism where the energy is extracted from a rotating black hole.

Expressions for the jet luminosity (in ergs/sec) in the two cases are:

$$BR : L = 1.6 \times 10^{38} (\frac{r_0}{r_g})^{3/2} B_8^2$$

$$BZ : L = 1.0 \times 10^{35} (\frac{J}{J_{max}})^2 (\frac{M}{M_\odot})^2 B_8^2$$

where r_0 is the inner radius of the disk, J the angular momentum of the black hole ($= J_{max}$ for a maximally rotating black hole) and B_8 the magnetic field at the inner disk radius in units of 10^8 G. For the given jet power and a maximally rotating 10 M$_\odot$ black hole we get $B = 6 \times 10^5$ G for BP and 3×10^7 G for BZ, both within range of expected fields derived earlier for the base of the jet. Other mechanisms may be important (e.g. Meier this conference) especially if an unstable state is reached with sporadic jets produced when the system changes to high/soft state.

4. Conclusions

We have found an apparently one-sided jet $\sim$ 30 au long in Cygnus X-1. The appearance is consistent with a Doppler boosted twin jet at 0.78c at around 40 degrees to the line of sight. A large proper motion $\gg$ beam size during the few hours of the observing runs is expected for such a velocity, so the jet image must be smeared. Multiple short snapshot observations are required to see if features do in fact move through the jet at the expected high proper motion. However these images will have lower signal to noise and have poorer mapping fidelity.

Standard jet production mechanisms for steady jets can produce the power required for a relativistic jet.

We note that the kink in the jet stays at a constant position; if this indeed indicates lack of motion along the jet then the jet is slow and must be intrinsically one-sided, and all the calculations above would have to be revised. Further observations are required to verify this feature.

It would be interesting to find the status of the jet when the source flares in the radio and in the transition to the high/soft X-ray state. Comparison with other episodic jet sources suggests that the jet should appear blobby and have a steep spectrum during this phase.

5. References

Blandford, R. D., and Königl, A. *Astrophys. J.*, 232, 34, 1979
Blandford, R. D. and Payne, D. G.,*Mon. Not. R. Astron. Soc.,* 199, 883, 1982
Blandford, R. D. and Znajek, R. L., *Mon. Not. R. Astron. Soc.,* 179, 433, 1977
Braes, L. L. E., and Miley, G. K., *Nature*, 232, 246, 1971
Brocksopp, C. et al. *Mon. Not. R. Astron. Soc.*, 309, 1063, 1999
Dhawan, V., Mirabel, I. F., and Rodriguez, L. F., *Astrophys. J.*, in press, astro-ph/0006086, 2000
Fender, R. P., et al. *Mon. Not. R. Astron. Soc.*, 304, 865, 1999
Fender, R. P., et al. *Mon. Not. R. Astron. Soc.*, 312, 853, 2000a
Fender, R. P., *Mon. Not. R. Astron. Soc.*, in press, astro-ph/0008447, 2000b
Hjellming, R. M. and Wade, C. M., *Astrophys. J. (Lett)*, 168, L21, 1971
Hjellming, R. M. and Johnston, K. J., *Astrophys. J.*, 328, 600, 1988
Mirabel, I. F. and Rodriguez, L. F., *Ann. Rev. Ast. & Astrop.* 37, 409, 1999
Stirling, A. M., Spencer, R. E., and Garrett, M. A., *New Ast. Rev.*, 42, 657, 1998
Stirling et al. *Mon. Not. R. Astron. Soc.*, submitted 2000

Magneto-rotational mechanisms of jet formation.

G.S. Bisnovatyi-Kogan (gkogan@mx.iki.rssi.ru)
Space Research Institute, Profsoyuznaya str. 84/32, Moscow 117810, Russia

Abstract. The magneto-rotational mechanism of jet formation in stationary and non-stationary events is analyzed. Collapse of a rotating magnetized body during star formation or supernovae explosion may lead to a jet-like mass ejection for certain angular velocity and magnetic field distributions at the beginning of the collapse.

Keywords: jet, magnetic field, rotation

1. Introduction

Matter outflow is observed in most astrophysical objects in the form of stellar wind, or collimated outflow (ejection) from young stellar objects, AGN and quasars, microquasars (galactic X-ray sources). Mechanisms of mass loss are connected with a radiative and/or electromagnetic acceleration. The last one, which is probably the best for producing collimated outflows, may work quasi-stationary, or may be connected with explosive events. Rotation is always present in compact objects, and formation of collimated jets results from the action of magneto-rotational phenomena.

2. Problem of collimation

During accretion and outflow of matter the relative dynamical action of magnetic field increases for a given element of matter. As was shown by Schwartzman (1971), the conservation of a magnetic flux during stationary accretion implies a dependence $B_r \sim r^{-2}$. At constant mass flux $\dot{M} = 4\pi\rho v_r r^2$ and free-fall velocity $v_r \sim r^{-1/2}$, the density increases as $\rho \sim r^{-3/2}$, and kinetic energy density $E_k \sim r^{-5/2}$. The growth of the magnetic energy density is faster $E_m \sim B_r^2 \sim r^{-4}$. After equipartition $E_k \sim E_M$ is reached, it cannot be violated during subsequent accretion.

The outflow from rotating magnetized object contain azimuthal component of the magnetic field, which energy density decreases not faster than the specific kinetic energy of matter. For the outflow with constant velocity v_r in stationary spherical outflow the density $\rho \sim r^{-2}$, $B_\phi \sim r^{-1}$. In this conditions $E_k \sim E_m$, and the trajectories of mass outflow become more tightly spiraled, and finally the flow is becoming highly collimated with direction of the flow along the rotational axis

(Heyvaerts and Norman, 1989; Bogovalov, 1998). We may say here about the universal magnetic collimation in the outflows from rotating magnetized objects.

The outbursts may be collimated at the very beginning. When jets are separated from the object of its origin the problem appears of preservation of the jet against its spherization during a motion in a rarefied medium. One of the plausible mechanism of jet preservation is a magnetic pinch collimation produced by an axial electrical current, suggested by Bisnovatyi-Kogan et al. (1969).

3. Jet formation by matter outflow from magnetized accretion disk

Accretion of matter with a large scale magnetic field into a black hole leads to formation of an accretion disk with a strong poloidal magnetic field. Models of non-rotating accretion disks, supported by magnetic field had been constructed by Bisnovatyi-Kogan and Ruzmaikin (1974, 1976). Rotation of matter in such a disk is accompanied by generation of a strong electrical field, leading to particle acceleration and ejection of matter along magnetic field lines. Qualitative and phenomenological models had been considered by Bisnovatyi-Kogan and Blinnikov (1976), Blandford (1976), Lovelace (1976). Analytical self-similar solutions for jets and winds produced by centrifugally and magnetically driven mechanisms had been obtained by Blandford and Payne (1982), Lovelace et al. (1991),

Extensive numerical simulations have been done for construction of more realistic models of quasi-stationary jet formation from magnetized accretion disks. In the paper of Romanova et al. (1998) have been done numerical simulations of dynamics of magnetic loops in the coronae of accretion disks. It was obtained that in presence of differential rotation the loops are opened in the inner parts of the disk, and opening of loops is followed by magnetically driven outflow from the disk. The outflow may be transient, consisting of small-scale outbursts from different loop opening, or may be steady, corresponding to outflow along the open field lines at the inner part of the disk, and showing some collimation. Computations of magnetocentrifugally driven winds had been performed by Ustyugova et al. (1999). The stationary regime of the outflow was obtained by solution of time-dependent MHD equations, with a split-monopole poloidal field configuration frozen into the disk. Close to the disk the outflow is driven by by the centrifugal force, while at all larger distances the flow is driven by the magnetic force, which is proportional to $-\nabla(rB_\phi)^2$, where B_ϕ is the toroidal field. The collimation distance over which the flow becomes collimated is much larger than the size of the sumulation region, so the obtained outflows are approximately spherical.

MHD simulation have been performed by Ustyugova et al. (2000) of Pointing outflows, where the mass flux is negligible and energy and angular momentum are carried predominantly by electromagnetic field in the form of MHD waves. As a result of time-dependent simulations a quasi-stationary collimated Pointing jet arises from the inner part of the disk and a steady uncollimated hydromagnetic outflow from the outer disk for a case Keplerian disk initially threaded by a dipole like poloidal magnetic field.

4. Magnetorotational explosions

A mechanism of producing magnetorotational explosion was suggested by Bisnovatyi-Kogan (1970), where amplification of the toroidal component of the magnetic field due to differential rotation leads to the transformation of a part of the rotational energy to the energy of the ejection. First numerical simulations devoted to the magnetorotational mechanism were made by Le Blanc and Wilson (1970). and investigated analytically by Meier et.al. 1976.

One of the most important parameters for this problem is relation of magnetic energy to the gravitational energy of the star: $\alpha = \frac{E_{\rm mag}}{|E_{\rm grav}|}$. Simulations have been done by Ardeljan et al. (2000). for the initial values of the $\alpha = 10^{-2}, 10^{-4}, 10^{-6}$. Details of the definition of the initial magnetic field are described in the paper by Ardeljan et al. (2000).

Initial magnetic field chosen for our simulations has quadrupole-like kind of symmetry (i.e. its "z"- component is equal to zero at the equatorial plane). As a result an ejection predominantly in the equatorial plane was obtained. The toroidal magnetic field grows with time and produces MHD shock which moves to the boundary of the star. Part of the matter of the envelope of the star (about 7% of the mass of the star) has radial kinetic energy larger than its potential energy and can be ejected. This ejected matter carries about 3.3% of the total energy of the star (see also poster PV-06). When the initial magnetic field have a dipole-like symmetry jet formation is possible as was shown in calculations of Le Blanc and Wilson (1970).

There is a possibility of asymmetric MHD explosion, when we have asymmetric magnetic field amplification. One example of development of asymmetric picture was considered by Bisnovatyi-Kogan and Moiseenko (1992). When the collapsing and exploding star has initially toroidal and poloidal fields of different symmetry: dipole poloidal and symmetric poloidal, or quadrupole poloidal and antisymmetric toroidal fields, formation of an additional toroidal field from the existing poloidal due to differential rotation leads to spontaneous breaking of the symmetry. Due to the asymmetry of the toroidal field during the explosion the outbursts could also become asymmetric, giving observational asymmetric or even one-side jets often observed in extragalactic jets, and may be in microquasars (Mirabel et al., 1992; Fender, 1999).

Acknowledgements

I am grateful to Dr. A.Castro-Tirado for hospitality, RFBR for partial support by grants 98-01-00352, 99-02-18180 and ESA-INTAS grant No.120.

References

Ardeljan, N. V., Bisnovatyi-Kogan, G. S., Moiseenko, S. G. *A&A*, **355**, 1181-1190, 2000.

Bisnovatyi-Kogan, G. S. *Astron. Zh.*, **47**, 813-816, 1970.

Bisnovatyi-Kogan, G. S., Blinnikov, S. I. *Pisma Astron. Zh.*, **2**, 489-493, 1976.

Bisnovatyi-Kogan, G. S., Komberg, B. V., Friedman,A. M. *Astron. Zh.*, **46**, 465-471, 1969.

Bisnovatyi-Kogan, G. S., Moiseenko, S. G. *Astron. Zh.*, **69**, 563-571, 1992.

Bisnovatyi-Kogan, G. S., Ruzmaikin, A. A. *Astrophys. Sp. Sci.*, **28**, 45-58, 1974.

Bisnovatyi-Kogan, G. S., Ruzmaikin, A. A. *Astrophys. Sp. Sci.*, **42**, 401-425, 1976.

Blandford, R. D. *Mon. Not. RAS*, **176**, 465-481, 1976.

Blandford, R. D., Payne, D.G. *Mon. Not. RAS*, **199**, 883-903, 1982.

Bogovalov, S. V. *Pisma Astron. Zh.*, **24**, 381-392, 1998.

Fender, R.P. *astro-ph/9907050*, 1976.

Heyvaerts, J., Norman, C. A. *ApJ*, **347**, 1055-1081, 1989.

Le Blanc, L. M., Wilson, J. R. *ApJ*, **161**, 541-551, 1970.

Lovelace, R. V. E. *Nature*, **262**, 649-652, 1976.

Lovelace, R. V. E., Berk, H. L., Contopulos, J. *ApJ*, **379**, 696-705, 1991.

Mirabel, I.F., Rodriguez, L.F., Cordier, B., Paul, J., Lebrun, F. *Nature*, **358** 215-217, 1992.

Meier, D. L., Epstein, R. I., Arnett, W. D., Schramm, D. N. *ApJ*, **204**, 869-878, 1976.

Romanova, M. M., Ustyugova, G. V., Koldoba, A. V., Chechetkin, V. M., Lovelace, R. V. E. *ApJ*, **500**, 703-713, 1998.

Schwartzman, V. F. *Astron. Zh.*, **48**, 479-488, 1971.

Ustyugova, G. V., Koldoba, A. V., Romanova, M. M., Chechetkin, V. M., Lovelace, R. V. E., *ApJ*, **516**, 221-235, 1999.

Ustyugova, G. V., Lovelace, R. V. E., Romanova, M. M., Li, H., Colgate, S.A. *ApJ*, **516**, 221-235, 2000.

MHD jets around galactic objects

Fabien Casse* and Jonathan Ferreira
Laboratoire d'Astrophysique de l'Observatoire de Grenoble, BP 53 F-38041 Grenoble cedex 9, France

Abstract. We present a self-similar, steady-state model describing both a magnetized accretion disc and a magnetohydrodynamic jet. We focus on the role of a hot corona in such a structure. This corona enables the disc to launch various types of jets. By considering the energy conservation, we also present a diagnostic of the luminosity of the magnetized disc, which could explain some observational signatures of galactic objects.

Keywords: magnetohydrodynamics (MHD), accretion disk

1. The disc-jet connection

In the Universe, jets of matter are observed around almost every kind of systems where plasma accretes onto a central object. The central object can be a young protostar, a compact galactic object or a supermassive black hole. The jet velocity is always found to be a few times the escaping velocity of the central object (e.g., Livio, 1997). The most successful model, accounting for all known properties of observed jets, relies on a large scale magnetic field anchored on an accretion disc (Blandford & Payne, 1982). The field extracts the disc angular momentum, thereby allowing accretion, and accelerates a fraction of disc material to high speeds. Moreover, the magnetic field confines the accelerating jet matter, leading to a cylindrical collimation of the jet. Hereafter, such systems are called Magnetized Accretion-Ejection Structures (MAES).

In a MAES, the bipolar magnetic field pinches *the disc*. Thus, the only force able to counteract both the magnetic and gravitational forces, *whithin the disc*, is the vertical plasma pressure gradient. As a consequence, the mass loading in the jet depends critically on this vertical equilibrium. This equilibrium is the connection between the accretion motion and the jet. A more detailed explaination of this phenomenon is displayed in Casse & Ferreira (2000a).

* Fabien.Casse@obs.ujf-grenoble.fr

2. Entropy generation

In all previous studies dealing with magnetized accretion disc steadily launching jets, the energy equation was simply disregarded. It was replaced by the assumption of isothermal or adiabatic magnetic surfaces. In the turbulent disc however, some physical mechanisms (convection, turbulent thermal conductivity) could provide a non-local energy transport, more efficent than by photons. We can mimic these effects by the following equation

$$\rho T \frac{dS}{dt} = Q$$

where Q is the difference between local heating and cooling rates of the plasma. This function Q is prescribed according to the energy conservation (Casse & Ferreira , 2000b). In a steady-state framework, this equation can be written as

$$Q = \frac{\gamma}{\gamma - 1} \frac{k_B}{m_p} \rho \vec{u_p} \cdot \vec{\nabla} T - \vec{u_p} \cdot \vec{\nabla} P \ .$$

where T is the temperature, P the plasma pressure, u_p the poloidal velocity of matter and γ the polytropic index of plasma. Because the gradient of plasma characteristics are almost vertical in a thin disc, one can see that entropy generation will have a strong impact on the vertical mass flux when the poloidal velocity is vertical (i.e. in the corona taking place at the disc surface). In the disc, the entropy generation will be advected with the flow onto the central object.

This is an important point since advection-dominated accretion flows (ADAF) only occurs in thick or slim discs ($h/r > 0.3$). Here, most of the entropy is generated in the disc atmosphere and taken in the jet, allowing the disc to be thin. Using this approximate form of the energy equation, we solve the full set of MHD equations from the disc midplane (resistive MHD regime) to the jet asymptotics (ideal MHD regime).

3. Global energy conservation

The global energy conservation enables us to know that the power released by accretion P_{acc} is shared between the total jet power P_{jet} (MHD Poynting flux, kinetic energy and enthalpy) and the disc luminosity L_D. We measure the amount of entropy generated with a parameter f whose value is determined by the disc turbulence ($0 < f \leq 1$). It is noteworthy that, according to the amount of entropy, the

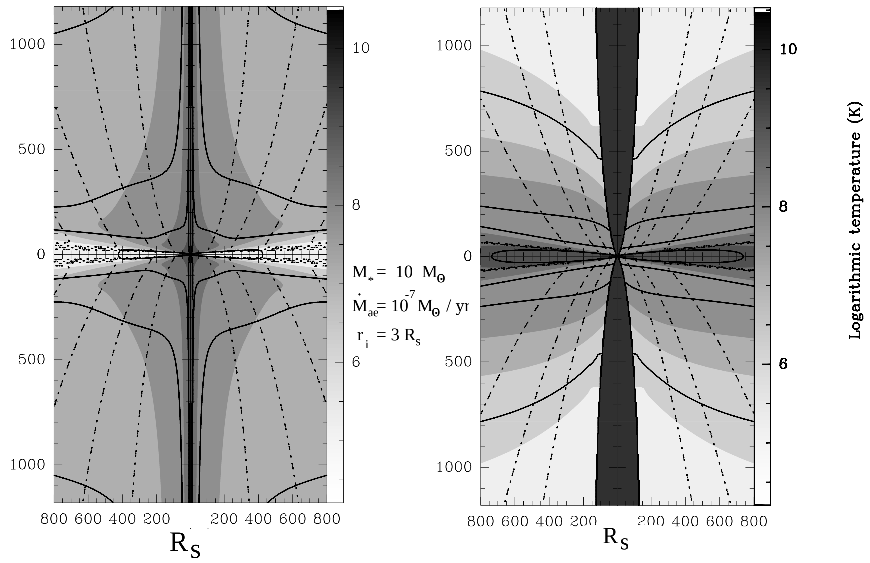

a. X-ray low/hard state ($f \to 1$)
Low disc emission & hot corona
Dense hot emitting jet

b. X-ray high/soft state ($f \to 0$)
Disc radiation & no coronal emission
Tenuous, cold and low emitting jet

Figure 1. Poloidal cross-section of MAES. In grey are shown the logarithmic temperature levels, the solid lines are the logarithmic plasma density levels ($\log n_H$ =12,12.5,13,15 in cm^{-3} for left pannel and $\log n_H$ = 9,10,11,15 for right pannel). The denser level is closer to the disc. The dashed lines represent plasma streamlines coming from the disc to the jet. The poloidal magnetic field lines are not displayed here but are strictly parallel, in the jet, to the poloidal streamlines, according to MHD equations. The left figure displays a structure that might be able to describe the X-ray low/hard state of some microquasars (see Fender et al., 1999). The right pannel could correspond to a X-ray high/soft state.

resulting jet is magnetically-driven ("cold" jet $f \sim 0$) or magneto-thermally-driven ("hot" jet $f \sim 1$). The energy conservation becomes (Casse & Ferreira , 2000b)

$$2L_D = (1-f)P_{diss} = P_{acc} - 2P_{jet}$$

where P_{diss} is the viscous and ohmic heating integrated all over the disc. One can easily see that if most of heat is deposited as entropy in the corona, a thin magnetized disc could launch jets and have a weak luminosity. Assuming the disc to be optically thick, we can calculate its luminosity L_D and effective temperature T_{eff}, namely

$$\frac{L_D}{L_{EDD}} \simeq 0.36 \left(\frac{1-f}{1+\Lambda}\right) \left(\frac{\dot{M}_{ae}}{10^{-7} M_\odot/yr}\right) \left(\frac{M_*}{10 M_\odot}\right) \left(\frac{3R_s}{r_i}\right)$$

$$kT_{\rm eff} \simeq 1{\rm keV} \left(\frac{1-f}{1+\Lambda}\right)^{\frac{1}{4}} \left(\frac{\dot{M}_a(r)}{10^{-7}M_\odot/yr}\right)^{\frac{1}{4}} \left(\frac{M_*}{10M_\odot}\right)^{-\frac{1}{2}} \left(\frac{r}{3R_s}\right)^{-\frac{3}{4}}$$

where we have assumed the external radius r_e of the MAES to be much larger than the internal radius r_i ($R_s = 2GM_*/c^2$ and L_{EDD} is the Eddington luminosity). The parameter Λ is the ratio of the magnetic to the viscous torque at the disc midplane and depends on the local MHD turbulence (Casse & Ferreira, 2000a).

An important consequence arises from these estimates. Indeed a magnetized disc driving jets could be less luminous than a standard accretion disc, even with $f \simeq 0$ (no corona). This will be the case if the turbulence is such that the magnetic torque is larger than the viscous one, the disc will be darker but keeping almost the same effective temperature.

In a stationary MAES, the characteristic timescale for jet launching is only a few dynamical timescales, i.e. roughly one second around a stellar black hole. So both low and high state of microquasars (e.g. Mirabel et al., 1998, Fender et al., 1999) might be described by two different MAES. Indeed the high state exhibits a strong thermal emission in X-rays (soft X-rays emitted from the disc, $f \to 0$) and a very small radio emission that could be accounted by a very tenuous, cold jet (or no jet at all). At the opposite, the low state is characterized by a non-thermal emission in hard X-rays (associated with a corona) and a "radio" jet. This low state might be obtained with a MAES where most of the heat is not released as radiation by the optically thick disc but shared between coronal losses and thermal energy sent into the jet ($f \to 1$). The resulting jets are hot and dense, and may be associated with a radio and infra-red emissions. In Figure 1, we display these two MAES. Anyway, a disc instability allowing the MAES to shift between these two states remains to be found. Also, to clearly validate this scenario, a modelisation of spectrum emitted from MAES must be performed and compared to observations. The authors would like to thanck Rob Fender for fruitful discussions.

References

Blandford, R.D. and Payne, D.G., 1982, *MNRAS* Vol.199 pp. 883
Casse, F. and Ferreira, J., 2000a, *A&A* Vol.353 pp. 1115-1128
Casse, F. and Ferreira, J., 2000b, *A&A* Vol.361 pp. 1178-1190
Fender et al., 1999, *ApJ* Vol.519 pp. L165-L168
Livio, M., 1997: "The formation of astrophysical jets" *ASP conferences series* Vol.121, Wickramasinghe T., Ferrario L., Bicknel, G.V.(eds.), p.845
Mirabel et al., 1998, *A&A* Vol.330 pp. L9-L12

On the Formation of Accretion-powered Galactic and Extra-galactic Outflows

Tapas K. Das
IUCAA Post Bag 4 Ganeshkhind Pune 411 007 INDIA (tapas@iucaa.ernet.in)

Abstract. Though widely observed to be emanating from a variety of astrophysical sources, the underlying physical mechanism behind the formation of galactic and extragalactic outflows is still enshrouded in a veil of mystery. In addition, it has not been possible to calculate accurately the amount of matter expelled in these events. In this article we present a *non-self-similar analytical model*, which, for the first time, we believe is able to explain the outflow formation phenomenon as well as compute the mass outflow rate by simultaneously solving the equations governing the exact transonic accretion and outflow. Our model predicts the dependence of this rate on various flow parameters as well as indicates the *exact* location from where the outflows are launched.

Keywords: AGN, quasar, microquasar, jet, accretion, accretion disk, black hole physics, hydrodynamics, outflow, wind, shock wave

1. Introduction

It is now a well established fact that quasars and microquasars suffer massloss through outflows and jets (Mirabel & Rodriguez 1999, Ferrari 1998, Begelman, Blandford & Rees 1984). These galactic and extra-galactic jet sources are commonly believed to harbour accreting compact objects at their hearts as the prime movers for almost all non-stellar energetic activities around them including the production of bipolar outflows and relativistic jets. Unlike normal stellar bodies, compact objects do not have their own physical atmosphere from where matter could be ripped off as winds, hence outflows from the vicinity of these prime movers *have to be generated only from the accreting material.* Instead of separately investigating the jets and accretion processes as two disjoint issues around the dynamical centre of the galactic and extra-galactic jet sources, it is absolutely necessary to study these two phenomena within the same framework and any consistent theoretical model for jet production should explore the outflow formation only from the knowledge of accretion parameters. Note that while self-similar models are a valuable first step, they can never be the full answer, and indeed any model which works equally well at all radii is fairly unsatisfactory to prove its viability. Thus the preferred model for jet formation must be one which is able to select the *specific* region of jet formation. Keeping these basic facts in our mind, we propose a *non self-similar analytical model* capable of self-consistently exploring the hydrodynamic origin of accretion powered jets/outflows emanating from galactic and extragalactic sources. Using this model it has been possible to simultaneously solve the accretion and wind equations to compute (from first principle) what fraction of accreting material is blown as wind and the exact location (distance from the central accretor) of the jet launching zone has been successfully pointed out.

Denoting $\dot{M}_{in}$ and $\dot{M}_{out}$ to be the instantaneous time rate of inflow and outflow around an accreting compact object, we define a quantity "Mass Outflow Rate ($R_{\dot{M}}$)" as the ratio of $\dot{M}_{out}$ to $\dot{M}_{in}$, which is basically a measure of the fraction of barionic accreting material being expelled as outflows/jets. Our major aim was to compute the exact value of $R_{\dot{M}}$ in terms of *minimum* number of accretion parameters and to investigate the dependence of $R_{\dot{M}}$ on various flow parameters. We do our calculation for accretion with considerable intrinsic angular momentum (Disc-Outflow system, see §2 for detail) and for spherical/quasi-spherical accretion with negligibly small angular momentum (see §3 for detail).

Because of the absence of any matter donating real physical atmosphere around accreting compact objects, we first need to incorporate some virtual surfaces around these objects from where outflows may be generated. Formation of these surfaces are explained in §2.1 (for the disc-outflow system) and in §3.1 (for spherical/quasispherical accretion-outflow system).

In this article, we are basically interested in highlighting the conceptual ideas behind our model rather than presenting the mathematical details, thus we keep this article free from any formulae or equations. Interested readers may kindly refer respective works (Das 1998, 1999, 1999a, 2000, 2000a, Das & Chakrabarti 1999 (DC99 hereafter)) for detail mathematical formalism.

2. The Disc-Outflow System

2.0. Model Description and Prescription for the Formation of Outflow Generating Surface

We consider thin, axisymmetric polytropic inflows around a Scwarzschild Black hole in vertical equilibrium. We ignore the self-gravity of the flow and calculations are done using Paczyński-Wiita (Paczynśki & Wiita, 1980) potential which mimics surroundings of the Schwarzschild black hole. Considering the inflow to be polytropic, we explore both the polytropic and the isothermal outflow.

Due to the fact that close to the BH the radial component of the infall velocity of accreting material would be enormously high, viscous time scale would be much longer than the infall time scale and a rotating inflow entering into a black hole will have almost constant specific angular momentum close to the black hole for any moderate viscous stress (Das, 1998 and DC99). Though at the outer edge of the accretion disk the angular momentum distribution may be Keplerian or even super-Keplerian, matter would be highly sub-Keplerian close to the black hole to satisfy the inner boundary condition at the event horizon of the BH (see Chakrabarti, these proceedings). This almost constant angular momentum produces a very strong centrifugal force which increases much faster compared to the gravitational force and becomes comparable at some specific radial distance, location of which is easy to compute. Here, (actually, a little farther out, due to thermal pressure) matter starts piling up and produces the centrifugal pressure supported boundary layer (CENBOL). Further close to the black hole, the gravity always wins and matter enters the horizon supersonically after passing through a sonic point. Formation of CENBOL may be attributed to the shock formation in accreting fluid or to the maximisation of polytropic pressure of the inflow. In CENBOL region the flow becomes hotter and denser and for all practical purposes behaves as the stellar atmosphere so far as the formation of outflows are concerned. A part of the hot and dense shock-compressed inflowing material is then 'squirt' as outflow from the CENBOL. In case where the shock does not form, regions around pressure maximum achieved just outside the inner sonic point of the *inflow* would also drive the flow outwards. The outflow is shown to be thermally and centrifugally accelerated but is assumed to be confined by external pressure of the ambient medium. Subsonic outflows originating from CENBOL would pass through sonic points and reach far distances as in wind solution.

2.0. The Overall Solution Scheme

Let us suppose that matter first enters through the outer sonic point and passes through a shock. At the shock, part of the incoming matter, having higher entropy density is likely to return back as winds through a sonic point, other than the one it just entered. Thus a combination of topologies, one from the region of accretion and the other from the wind region is required to obtain a full solution. In the absence of the shocks, the flow is likely to bounce back at the pressure maximum of the inflow and since the outflow would be heated by photons, and thus have a smaller polytropic constant, the flow would leave the system through an outer sonic point different from that of the incoming solution. By simultaneously solving the proper set of equations in appropriate geometry (see Das, 1998, DC99 and Chapter 2.1 & 2.2 of Das, 2000a for detail solution scheme and flow geometry), we get the *combined* flow topologies (Fig 2. of DC99) where the value of $R_{\dot{M}}$ along with *all* other outflow parameters can be exactly computed only from the knowledge of the *minimum number of* accretion parameters namely specific energy ($\mathcal{E}$), specific angular momentum (λ), accretion rate (scaled in the unit of Eddington rate) ($\dot{M}_{in}$) and adiabatic indices (γ) of the flow. Also the dependence of $R_{\dot{M}}$ on *all possible* flow parameters has been investigated self-consistently (see Das, 1998 and DC99 for detail).

3. Outflows from Spherical/Quasi-spherical Accretion

3.0. The Outflow Generating Surface

For this class of accretion, absence of angular momentum rules out the possibility of formation of CENBOL. A novel mechanism is present in the literature (Kazanas & Ellison 1986, Protheroe & Kazanas 1983) where the kinetic energy of spherically accreting material has been randomized by proposing a steady, standing, collisionless, relativistic hadronic pressure supported spherically symmetric shock around a Schwarzschild black hole which produces a nonthermal spectrum of high energy (relativistic) protons. A fraction of the energy flux of infalling matter is assumed to be converted into radiation at the shock standoff distance through hadronic ($p-p$) collision and mesonic ($\pi^{\pm}, \pi^0$) decay. Pions generated by this process, decay into relativistic electrons, neutrinos/antineutrinos and produces high energy γ rays. These electrons produce the observed non-thermal radiation by Synchrotron and inverse Compton scattering. Shock accelerated relativistic protons are not readily captured by the black hole rather considerable high energy density of these relativistic protons would be maintained to make this shock self-supported (Protheroe & Kazanas, 1983). In this work, we take this pair-plasma pressure mediated shock surface as the alternative of the CENBOL from where the outflow could be launched.
Here we consider that a Schwarzschild type black hole quasi-spherically accretes fluid obeying polytropic equation of state. We also assume that for our model, the effective thickness of the shock is small enough compared to the shock standoff distance. We investigate polytropic as well as isothermal outflows from polytropic accretion.

3.0. The Overall Solution Scheme

The *exact* value for the shock location and all relevant pre- and post-shock quantities can be computed in terms of $\mathcal{E}, \dot{M}_{in}$ and γ. Now using the the slountion scheme as described for the disc-outflow system, the set of equations are simultaneously solved in proper geometry to get the combined flow topology for polytropic and isothermal outflows (see Das 1999, 1999a, 2000 for detail solution scheme and flow geometry) where $R_{\dot{M}}$ along with *all other* outflow parameters was calculated and its dependence on all flow parameters has been studied.

4. Some Important Results and Directions for Future Work

4.0. Explanation of Quiescent States of X-ray novae

An interesting situation arises in our model when the polytropic index of the outflow is large and the compression ratio is also very high. In this case, the flow virtually bounces back as the wind and the outflow rate can be equal to the inflow rate or even higher, thereby evacuating the disk completely (see Fig. 6 of Das, 1998). These cases can cause runaway instabilities by rapidly evacuating the disk. It is possible that some of the black hole systems, including that in our own galactic centre, may have undergone such evacuation phase in the past and gone into quiescent phase. Thus our model could explain the quiescent states in X-ray novae systems like GS 2000+25 or GRS 1124-633 etc. (Tanaka 1995, Ueda et al, 1994) and also in some systems with massive black holes, especially the black hole at our galactic centre.

4.0. Spectral Properties of Our Galactic Centre

We suggest that (Das 1998, Das 2000a, DC99) a possible explanation for extreme low luminosity and low radiative efficiency (upper limit on the mass accretion rate of $SgrA^*$ is of the order of $\sim\ 8 \times 10^{-5}\ M_\odot\ Yr^{-1}$, Bondi accretion rate on it has been approximated as $\sim\ 3\times 10^{-5}\ M_\odot\ Yr^{-1}$ (Quarteart, Narayan & Reid 1999 and references therein)) could be due to the presence of profuse mass loss from the vicinity of $SgrA^*$. We found that for such low accretion rates the mass outflow rate is exorbitantly high, almost to the point of evacuating the disk, which prompted us to strongly speculate that the spectral properties of our galactic centre could be explained by inclusion of wind using our model. However, possibility that outflow in an accretion disk wind might explain the low accretion rate at the Galactic Center also has been suggested by Blandford & Begelman (1999).

4.0. Outflow Driven Contamination of Metalicity to the Outer Galaxies

A number of observational evidences suggest that the fluid accreting onto black hole has potential to generate appropriate temperature which supports significant nucleosynthesis to take place in accretion disks around black holes (Mukhopadhyaya & Chakrabarti, 1999 and references therein). It is interesting to investigate whether the fate of the shock induced nucleosynthesis generated heavier elements could be predicted by our disk-outflow model. One of the major speculations of our model (Das, 1998, DC99 and §5.1 of Chapter 2.2 of Das, 2000a) that outflows from the hot and dense CENBOL (where the composition change is much more significant) would carry away modified compositions and contaminate the atmosphere of the surrounding stars and galaxies in general. Strong indications of disk-evacuation by wind for some region of parameter space suggests (Das, 1998, DC99) that overall such contributions to metalicity must not be neglected. Significant work in this direction is in progress and is expected in near future.

Acknowledgements

I would like to thank the LOC of this workshop, and my special thanks goes to A. Castro-Tirado for kindly providing the financial assistance for attending the workshop.

References

Begelman, M. C., Blandford, R. D. & Rees, M. J. 1984. Rev. Mod. Phys. 56, 255
Blandford, R. D. & Begelman, M. C. 1999. MNRAS. 303, L1.
Das, T. K., 1998. in Observational Evidence for Black Holes in the Universe, Ed. S. K. Chakrabarti (Kluwer Academic: Holland). p. 113.
Das, T. K. 1999, Ind. Jour. Phys. 73(B), 1,1.
Das, T. K. 1999a, MNRAS. 308, 201.
Das, T. K. 2000. MNRAS. 318, 294.
Das, T. K. 2000a. Ph.D. Thesis.
Das, T. K. & Chakrabarti, S. K., 1999. Class. Quantum Grav. 16,3879. (DC99)
Ferrari, A. 1998. ARA&A. 36, 539.
Kazanas, D., Ellison, D. C., 1986, ApJ. 304 178.
Mirabel, I. F., & Rodriguez, L. F., 1999. ARA&A. 37, 409.
Mukhopadhyay, B. & Chakrabarti, S. K. 2000. A & A. 353, 1029.
Paczyński, B. & Wiita, P. J. 1980, A & A, 88, 23.
Protheroe, R. J., & Kazanas, D., 1983, ApJ, 256, 620.
Tanaka, Y., 1995, Nature, 375,659.
Ueda, Y., Ebisawam K. & Done, C. 1994, PASJ, 46, 107.

Jet Formation and Dynamics: Comparison of Quasars and Microquasars

Wolfgang Kundt
IfA of Bonn University, Auf dem Hügel 71, D-53121 Bonn

Abstract. Quasars and Microquasars share the following properties: (i) They have similar, elongated morphologies - reminiscent of being driven by supersonic beams - consisting of cores, knots, and heads, with jet-opening angles $\lesssim 10^{-2}$, and no beam branching; (ii) core/lobe power ratios of $10^{2\pm2}$; (iii) fluctuating, broad and hard core spectra; (iv) (occasional) sidedness; (v) (occasional) superluminal growth.

In all cases, the central engine is thought to be a rotating magnet whose reconnecting magnetic fields generate the relativistic pair plasma – of typical Lorentz factor $10^{3\pm2}$ – which rams the jet channels and blows the cocoons (subsonically) after having been stalled in a head. The supersonic jets form on passing a central deLaval nozzle, first proposed by Blandford and Rees in 1974, which forms naturally due to the huge density contrast of $10^{-8.3}T_4$ w.r.t. the ambient medium (of temperature T/10^4K). Beam stability and narrowness are likewise guaranteed by the density contrast (of jet fluid and CSM). Observed are both the (thermal) radiation of the rammed channel-wall material, and the synchrotron radiation of the deflected beam particles.

Keywords: bipolar flows, black hole candidates, jet dynamics, microquasar

1. Properties of the Jet Sources

At this workshop, an opinion has been repeatedly expressed – e.g. by Ralph Spencer and by Philippe Durouchoux in their discussions – that the obvious analogy between the (extragalactic) quasars and the (stellar) microquasars was perhaps more fundamental than expected from their modeling which allows for quite different *central engines*: young stellar objects, neutron stars, stellar-mass black holes, supermassive black holes, and quite different *jet compositions*: relativistic pair plasma [Kundt and Gopal-Krishna, 1980; Begelman et al, 1994], focussed stellar winds, fired bullets (plasmons). Christian Kaiser has pointed out difficulties of the plasmon model for jets. Wlodzimierz Kluzniak and Andrea Merloni have highlighted details of the X-ray power spectrum of black-hole candidates (BHCs) which prefer an interpretation via a neutron star (with a well-defined spin frequency, and hard surface). Rob Fender arrived at marginally tolerable beam energetics – using the measured spectra – by making the minimum assumption of pure pair plasma. And in his numerical modeling of jets, David Meier had increasing success with an increasing Lorentz factor of the beam particles.

All these results agree with the work by Gopal-Krishna and myself [1980], also by Blome and myself [1988], in which we conclude that the beam fluid must be relativistically light (and magnetized at pressure balance) in order for the jets to stay narrow, multiply focussed, and never branching and in order to conserve 4-momentum and particle number in the heads of the flows. Independently, I have never seen a robust mechanism of *jet formation* proposed other than the buoyant escape of some quasi-weightless fluid out of the deep potential well of the central engine. Also, I have repeatedly argued that the *stellar-mass BHCs* are binaries containing a neutron star inside a massive accretion disk (M $\approx 5M_\odot$), [Kundt and Fischer, 1989; Kundt, 1998b, 1999a]; black holes are in disharmony with the (i) hard spectra (up to γ-ray energies), (ii) (X-ray) luminosity maxima and minima, (iii) quasi periods, (iv) (noisy and asymmetric) lightcurves and line velocities, (v) pair-formation capability, and with various further details.

Microquasars received their name because their properties are quite similar to those of the quasistellar radio sources (quasars) and because their powers are over a million times weaker than those of the latter. This classification should include not only the jet-forming binary neutron stars and black-hole candidates (which were the main subjects of this workshop) but also the jet sources issuing from *binary white dwarfs*, and from *young stellar objects* (YSOs). The former are less obvious because hidden inside planetary nebulae; they were highlighted in [Kundt, 1996a] and have M1-92 [Trammell and Goodrich, 1996], He2-90, and CRL 618 as their presently clearest representatives. The latter include (young) expanding radio triples and one-sided nuclear radio jets [Kundt, 1996a, 1998a], and tend to have several successive heads so that they are much longer (several pc) than originally realized [Reipurth, 1997]. Finally, more and more jets are detected even from high-mass X-ray and γ-ray binaries, cf. [Paredes et al, 2000].

Talking about morphologies, a well-known dichotomy are the Fanaroff and Riley classes I and II of extragalactic radio sources with center- and edge-brightened cocoons, which have been recently redefined by Jean Eilek as of *type A and type B* depending on whether or not their head still ploughs supersonically into its surrounding medium [Kundt, 1999b]; class II is contained in type A. The new classification offers the prediction that all sources evolve from type A to type B as their ram pressure in the head tends to decrease with increasing source size (for constant injection power) whilst the ambient sound speed tends to increase (with increasing ambient temperature). Type A is statistically younger. This same dichotomy can be found in microquasars whereby a core-jet source can be easily misclassified as of type B before its distant heads have been identified.

2. Jet Fluid and Central Engine

Why do the microquasars deserve their name, i.e. behave like scaled-down quasars? How different are they from their mega counterparts? In this section I shall argue that indeed, their *formation mechanism* is basically the same: Magnetic reconnections – like on the sun – generate relativistic pair plasma whose buoyant escape from the central potential well rams two antipodal escape channels, perpendicular to the feeding disk, seen as two knotty jets. The big difference between the two source classes – beyond their vastly different power – is the density of their ambient media, $10^{2\pm3} cm^{-3}$ versus $10^{-5\pm2} cm^{-3}$, i.e. again a factor of $\gtrsim 10^6$, with the microquasars being embedded in *megadense* media.

Crucial in this comparison is the claim that all jet sources are driven by *pair plasma*, including the young neutron-star binary SS 433 [Kundt, 1996a, 1998b,c]. Here are six reasons to support this long-standing claim: • Pair formation via magnetic reconnections is a robust mechanism – demonstrated by flares on the sun – which is expected to take place abundantly around all magnetized rotators: young neutron stars, young white dwarfs, young stars, and the dense centers of galactic disks (s.b.). • Pair-plasma jets can perform an ordered, loss-free $\vec{E} \times \vec{B}$ drift (at practically equal velocities of both charges) – apart from unavoidable inverse-Compton losses – so that the (dubious) assumption of any downstream in-situ post acceleration is avoided [Kundt, 1998c]. Analogous examples from daily life are the electron beams illuminating a TV screen. • Our Galactic disk is an abundant emitter of the 511 keV pair-annihilation line, some $10^{43} s^{-1}$ annihilations, a rate that exceeds radioactive interstellar positron productions by a factor of $\gtrsim 30$ but which is expected from all the Galactic microquasars [Kundt, 1997]. • When compared with hadronic jets, pair-plasma jets require distinctly lower powers, just low enough to be consistent with the Eddington limit for stellar sources. • Pair-plasma jets can be destroyed by inverse-Compton losses on the photon flood from a nearby bright star (when unsuitably oriented), such as σ Orionis [Reipurth et al, 1998], or the companion in Cygnus X-1 [R. Spencer, these proceedings]. • Wardle et al [1998] have concluded at a pair-plasma composition of quasar beams from the presence of some 1% circular polarization and simultaneous presence of strong linear polarization which imply equal numbers of low-energy ($\gamma < 10^2$) electrons and positrons.

How different are the *central engines* of quasars and microquasars? If spinning stellar magnets are the engines of the latter, as argued above, what are their mega cousins? Zsolt Paragi called them 'black boxes'. In [1999b] I gave eight reasons of why I consider supermassive black holes inconsistent which I will repeat below; cf. [Hoyle et al, 2000]. My preference is for *burning disks*: mass densities $\rho(r)$ inside galactic disks grow as $r^{-2+2\epsilon}$ with decreasing distance r from the center, for a rotation curve $v(r) \sim r^{\epsilon}$, hence approach stellar values near the center. Even for an initially empty center, a typical galactic mass-spiral-in rate of $\lesssim M_{\odot}/yr$ guarantees that the innermost solar-system-sized parts of the disk fill up to nuclear-burning densities, on the timescale of Myrs. Such a central disk will be disrupted by nuclear detonations long (in density) before a black hole can form [1996b] and will be observed in the form of the BLR. Its vertical mass distribution reads $\rho(z)/\rho_c \approx 1/cosh^2(z/z_h)$ with $\rho_c \lesssim 10^2 g/cm^3$, $z_h = v_{th}/(2\pi G\rho_c)^{1/2} \lesssim 10^{10} cm$, and its Keplerian revolution velocities $\sqrt{\pi G\sigma r}$ can reach 0.1c [Pandey and Gupta, 1998; Kundt, 1999b]. Sgr $A^{\star}$ may have a present nuclear-burning disk radius of $10^{13.6} cm$.

Burning disks (BDs) might never have given supermassive BHs a chance as engine for an AGN had not Ed Salpeter [1971] expressed an early warning considering their stability, assuming radiation-pressure support without nuclear burning. On the other hand, here are the eight BH difficulties expressed in [1999b]: (i) a missing factor of 10^4 in the unresolved *core masses* of nearby galaxies (of $10^{6.5\pm3} M_{\odot}$: [Kormendy and Richstone, 1995]), on account of the integrated QSO light; (ii) on average, *mass-outflow* rates from AGN are not smaller than mass-inflow rates: $\dot{M}_{out}/\dot{M}_{in} \approx \beta_{-1} r_{16} N_{24.5}/L_{46}$; (iii) a BH is too *$\gamma$-ray compact* for the relativistic jet plasma to escape, not only in the case of the radio-quiet sub-population; (iv) BLR spectra are $\gtrsim 10^2$-times *metal enriched* over solar, like for the glowing ashes of nuclear fires [Turnshek, 1988]; (v) QSO *spectra* range all the way up to TeV energies and beyond, much too *hard* for a swallowing giant BH; (vi) the putative BHs *evolve invertedly* to the QSO phenomenon [1999b; cf. Schmidt et al, 1995, Richstone et al, 1998]; (vii) the *nuclear-burning hurdle* has prevented BH formation, by a margin in surface-mass density of $\lesssim 10^2$; (viii) the *universality* of the *bipolar-flow* phenomenon asks for a uniform engine: a spinning magnet which generates the indispensible non-thermal component (pair plasma).

The following table summarizes my understanding of the two discussed jet classes. Their differences may be solely due to the differences in source power and ambient density. To me, they look like the same physical phenomenon.

Table 1. Comparison of QSOs with microQSOs: Θ := beam opening angle, L_c/L_l = core/lobe power ratio, $\beta_\perp$:= (apparent) $v_\perp/c$, Ω := ρ_{amb}/ρ_{jet}. Note that $\gamma_{bulk} \geq \sqrt{1+\beta_{perp}^2}$ holds rigorously, due to special-relativistic kinematics.

source	Θ	$\frac{L_c}{L_l}$	spec-	-trum	γ	$\beta\perp$	sided	C.E.	Ω	radio loud	radio quiet
AGN	10^{-2}	10^2	$\lesssim$TeV	cont	$10^{3\pm2}$	$\lesssim 30$	more	BD	10^8	quasar	QSO
n $\star$	10^{-2}	10^2	$\lesssim$MeV	line	$10^{3\pm2}$	$\lesssim 5$	less	n $\star$	10^{12}	μquasar	μQSO

Acknowledgements

I should like to thank Hans Baumann, Ashok Singal, and Gernot Thuma for several joint seminars on the subject, Josep Paredes for constructive criticism, and Günter Lay for converting my writeup into something submittable.

References

Begelman, M. C., M. J. Rees, and M. Sikora. Energetic and radiative constraints on highly relativistic jets. *Astrophys. J.*, 429 :L57–60, 1994.

Blandford, R. D. and M. J. Rees. A 'Twin-Exhaust' Model for double Radio Sources. *Mon. Not. Royal Astron. Soc.*, 169 :395–415, 1974.

Blome, H.-J. and W. Kundt. Leptonic Jets from Young Stellar Objects. *Astrophys. and Space Sci.*, 148 :343–361, 1988.

Hoyle, F., G. Burbidge, and J. V. Narlikar. *A different Approach to Cosmology.* Cambridge University Press, 2000.

Kormendy, J. and D. Richstone. Inward Bound: The Search for Supermassive Black Holes in Galaxy Nuclei. *Ann. Rev. Astron. Astrom.* 33 :581–624, 1995.

Kundt, W. *Jets from Stars and Galactic Nuclei.* Lecture Notes in Physics 471, Springer, 1996a.

Kundt, W. Galactic Nuclei. *Astrophys. and Space Sci.* 235 :319–327, 1996b.

Kundt, W. Structure of the Galactic Halo and Disk. In H. Lesch, R.-J. Dettmar, U. Mebold, and R. Schlickeiser, editors, *The Physics of Galactic Halos*, pages 255–259. Akademie Verlag, Berlin, 1997.

Kundt, W. Jets from Stars and Galactic Nuclei. In S. Massaglia and G. Bodo, editors, *Astrophysical Jets*, pages 61–70. Gordon and Breach, 1998a.

Kundt, W. Astrophysics of Neutron Stars: Facts and Fiction about their Formation and Functioning. *Fundamentals of Cosmic Physics*, 20(1) :1–119, 1998b.

Kundt, W. The Gold Effect: Odyssey of Scientific Research. In A. Richter, editor, *Understanding Physics*, pages 187–240. Copernicus Gesellschaft, Katlenburg-Lindau, 1998c.

Kundt, W. The (stellar-mass) Black-Hole Candidates. In F. Giovannelli and L. Sabau-Graziati, editors, *Multifrequency Behaviour of High-Energy Cosmic Sources*, pages 1105–1110. *MEM.S.A.It.* Vol. 70 N. 3/4, 1999a.

Kundt, W. Radio Galaxies powered by Burning Disks. In J. Biretta and P. Leahy, editors, *Life Cycles of Radio Galaxies*, STSci Baltimore proceedings, submitted to Elsevier on 29 September, 1999b.

Kundt, W., and D. Fischer. Is there a Black Hole among the Black-Hole Candidates?. *J. Astrophys. Astron.*, 10 :119–138, 1989.

Kundt, W., and Gopal-Krishna. Extremely relativistic Electron-Positron Twin-Jets form Extragalactic Radio Sources. *Nature*, 288 :149-150, 1980.

Pandey, U. S. and A. C. Gupta. Equilibria of self-gravitating gaseous disks. *Bull. Astr. Soc. India*, 26 :731–737, 1998.

Paredes, J. M., J. Martí, M. Ribó, and M. Massi. Discovery of a High-Energy Gamma-Ray-emitting persistent Microquasar. *Science*, 288 :2340–2342, 2000.

Reipurth, B. Herbig-Haro Jets and their Role in Star Formation. *The Messenger*, 88 :20–26, 1997.

Reipurth, B., J. Bally, R. A. Fesen, and D. Devine. Protostellar Jets irradiated by massive stars. *Nature*, 396 :343–345, 1998.

Richstone, D. et al (14 authors). Supermassive black holes and the evolution of galaxies. *Nature* 395 :A14–A19, 1998.

Salpeter, E. E. Fragmentation of Supermassive Disks. *Nature Phys. Sci.* 233 :5–7, 1971.

Schmidt, M., D. P. Schneider, and J. E. Gunn. Spectroscopic CCD Surveys for Quasars at large redshift IV. Evolution of the luminosity function from quasars detected by their Lyα emission. *Astron. J.* 110 :68–77, 1995.

Trammell, S. R. and R. W. Goodrich. HST and ground-based Imaging of the bipolar proto-planetary nebula M1-92: evidence for a collimated outflow. *Astrophys. J.* 468 :L107–110, 1996.

Turnshek, D. A. BAL QSOs: Observations, Models and Implications for Narrow Absorption Line Systems. In J. C.Blades, D. A. Turnshek, and C. A. Norman, editors, *QSO Absorption Lines: Probing the Universe*, pages 17–51. Cambridge Univ. Press, 1988.

Wardle, J. F. C., D. C. Homan, R. Ojha, and D. H. Roberts. Electron-positron jets associated with the quasar 3C 279. Nature 395 :457–461, 1998.

Jet Dynamics and Emission

José-Luis Gómez
Instituto de Astrofísica de Andalucía (CSIC)
Apdo. 3004, Granada 18080, Spain

Abstract. Numerical relativistic hydrodynamical simulations have been recently used to study the dynamics of relativistic jets in active galactic nuclei and micro-quasars. Computation of the non-thermal emission from this hydrodynamical models have allowed a direct comparison with recent high resolution observations of these sources, revealing the important role this method can play in the understanding of the physical processes taking place in these sources. This paper reviews some of the latest results in numerical relativistic hydrodynamical and emission simulations of jets. Recent observations are also analyzed on the light of these simulations.

Keywords: relativistic jet, hydrodynamics, radiation mechanisms:non-thermal

1. Introduction

Over the past two decades there has been a significant effort to obtain a better understanding of the fluid dynamics in astrophysical jets through numerical simulations. First simulations, restricted to classical fluids dynamics, explored with great success the propagation and morphology of jets (see the reviews of Norman 1996 and Ferrari 1998). Application to relativistic flows began in the nineties (Martí, Müller, & Ibáñez 1994; Duncan & Hughes 1994; Martí et al. 1995, 1997; Komissarov & Falle 1998; Rosen et al. 1999; Aloy et al. 1999a), thanks to the development of new numerical techniques capable of solving the time-dependent equations of relativistic hydrodynamics for large flow Lorentz factors and strong shocks (see the review by Martí & Müller 1999).

Some of the latest simulations have started to explore three dimensional relativistic jets (Aloy et al. 1999a,b, 2000; Hardee 2000), magnetized relativistic jets (Komissarov 1999), as well as jet formation and collimation making use of the first general relativity magnetohydrodynamical codes (Koide, Shibata & Kudoh 1999; see also the review by Meier 2001). Computation of the non-thermal (synchrotron) radio emission from the hydrodynamical results (Gómez et al. 1995, 1997; Mioduszewski, Hughes & Duncan 1997; Komissarov & Falle 1997; Aloy et al. 1999b, 2000; Jones, Ryu & Engel 1999) allows a direct comparison with the observations through which test our models.

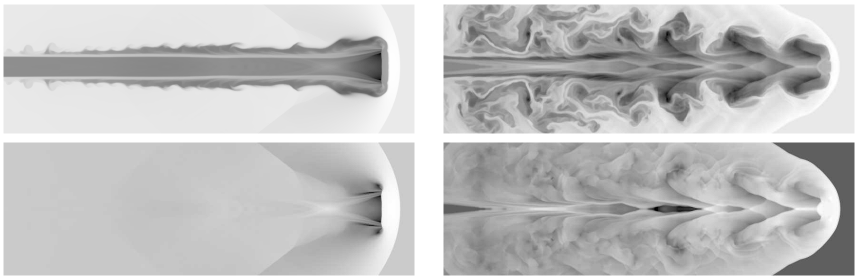

Figure 1. Numerical hydrodynamical simulations of a relativistically "hot" (*left*) and "cold" (*right*) jet (from Martí et al. 1997). Panels show the logarithm of the proper rest-mass density (top) and pressure (bottom).

2. Morphology of Relativistic Jets

The main differences that are expected to arise between the morphology of classical and relativistic jets come from the increase in the effective inertial mass of relativistic jets (Martí et al. 1995, 1997; Duncan & Hughes 1994), as can be deduced from the momentum equation. Relativistic implications in the jet morphology may be caused by relativistic flow speeds or relativistic internal energies. Martí et al. (1997; see also the review by Martí 2000) explored the main differences between hot jets (i.e., beams with internal energies comparable to the rest-mass energies), and highly supersonic ones (those in which the kinematic relativistic effects due to high jet Lorentz factors dominate).

Hot jets show little internal structure and relatively smooth cocoons (see Fig. 1). The lack of complex internal structures allows the terminal shock to remain well defined during the jet propagation through the external medium. Therefore, hot jets are expected to present a terminal hot spots, similar to those observed in Faranoff-Riley AGN type II sources. On the other hand, highly supersonic jet models, in which the high Lorentz factors dominate the kinematic relativistic effects, present a richer internal structure, with multiple internal shocks, and extended overpressured cocoons (Fig. 1).

Indications of the collision between the jet and external medium has been observed in several microquasars (Mirabel & Rodríguez 1999). For the superluminal microquasars GRO J1655-40 and GRS 1915+105, only the latter has been found to show some evidence for the existence of lobes, although the most plausible interpretation for the observed features is in terms of regular HII regions (Rodríguez & Mirabel 1999). Formation of terminal hot spots and lobes is determined by the jet momentum and the density contrast between the jet and external medium. Therefore, the apparently missing lobes in these two sources suggests that either both sources carry relatively small momentum, which would require cold and/or light jets (since they are the fastest jets observed in microquasars), or propagate through a light medium. Ejections in GRS 1915+105 and GRO J1655-40 are quite episodic, which may be an indication for light jets in both sources, or even the lack of continuous jets. This may therefore explain why no lobes or hot spots have yet be seen in these sources.

3. Relativistic HD and Emission Simulations

Computation of the synchrotron emission from the hydrodynamical models requires several assumptions. Firstly, the particle and energy density of the nonthermal emitting particles is considered to be a constant fraction of the thermal gas. Secondly, the hydrodynamical internal energy density has to be distributed among the emitting particles, which is usually done by assuming a power law energy spectrum (Gómez et al. 1995). Finally, it is still largely unknown what may be the role played by the magnetic field in the jet dynamics of AGNs and microquasars. There are some evidence pointing towards a small contribution of the magnetic field in the dynamics (Hughes 2000), although only future observations and magnetohydrodynamical simulations (van Putten 1993; Komissarov 1999; Koide, Shibata, & Kudoh 1999) could answer this question. So far, and mainly due to the fact that the emission computations have been performed for purely hydrodynamical models, the magnetic field has been assumed to be dynamical negligible. In this case, ad-hoc magnetic field structures are considered, with an energy density proportional to the fluid pressure.

The presence of emitting gas at velocities close to that of the speed of light enhance the importance of the relativistic effects in the final emission structure of the simulated maps. Besides light aberration (Doppler boosting), time delays is the most important effect determining the final emission structure (no superluminal motions can be obtained from these simulations without considering the time delays between different jet regions). Once the absorption and emission coefficients are determined (accounting for the retarded times), the transfer equations for the synchrotron radiation are solved along the line of sight, allowing the computation of simulated intensity maps.

3.0. Relativistic Shocks

Shock-in-jet models (Marscher & Gear 1985; Hughes, Aller, & Aller 1985) have been proven to provide a general explanation for the emission variability observed in components of relativistic jets. Numerical

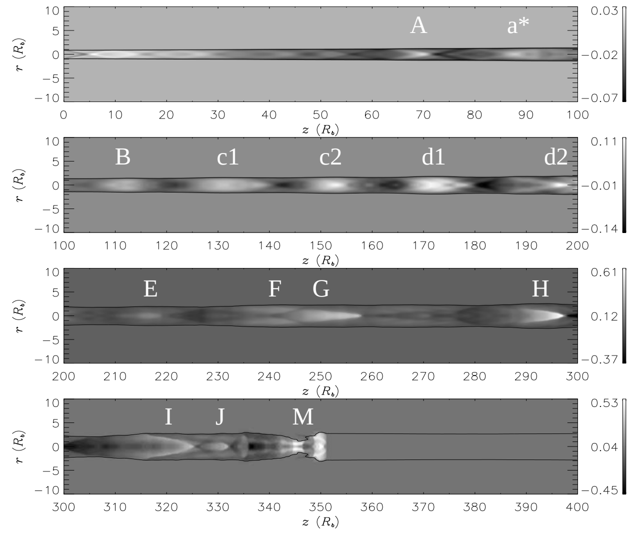

Figure 2. Relative variation with respect to the undisturbed steady jet of the Lorentz factor (logarithmic scale) for a jet in which a perturbation in Lorentz factor was introduced at the jet inlet. The panels show the appearance of multiple conical shocks (labeled "A" to "J") trailing the main shock ("M") produced by the perturbation.

relativistic HD and emission simulations provide a new powerful tool to improve upon these previous analytical models. With these new numerical techniques it is now possible to study with great detail the generation, structure, and evolution of strong shocks, and analyze its importance in the overall dynamical evolution and emission of jets through comparison with recent high resolution VLBI observations.

In the models presented by Gómez et al. (1997), Komissarov & Falle (1997), and Mioduszewski, Hughes, & Duncan (1997), superluminal components are obtained from perturbations in steady relativistic jets. In Gómez et al. (1997) the introduction of a short living square-wave perturbation in the flow Lorentz factor (from an initial value of 4 to 10) is observed to quickly evolve into a traveling shock followed by a rarefaction of slower flow. Because of the enhanced pressure in the shocked plasma, these shocks appear in the simulated intensity maps as regions of increased emission moving downstream at superluminal apparent velocities.

The evolution of the shocked plasma is determined by its interaction with the external medium as well as the underlying jet, which was neglected in the previous simplified analytical models. This results in the appearance of an internal changing structure in the shocked plasma. Time delays stretches the emitting region in the observer's frame, amplifying this inhomogeneities and leading to the appearance of discrete knots within the superluminal component associated with the shocked plasma (Gómez et al. 1997). Furthermore, the passage of the shock wave triggers a local pinch instability that leads to the formation of a series of conical trailing shocks (Agudo et al. 2001a,b) that follow the main shock (Fig. 2). These trailing shocks can be easily distinguished because they appear in the simulated maps as components being released on the wake of primary superluminal component (associated with the leading shock), instead of being ejected from the core of the jet. Those trailing components appearing closer to the core show small apparent motions and a very slow secular decrease in brightness, from which they could be identified as stationary components. Those appearing farther downstream are weaker and can reach superluminal apparent motions. Their oblique nature should also result in different polarization properties from that of the main planar leading shock. The existence of these trailing components indicates that not all observed components necessarily represent a major perturbation at the jet inlet; rather, multiple emission components can be generated by a single disturbance in the jet.

4. Comparison with Observations

High resolution millimeter VLBI observations have confirmed some of the above mentioned results. In the radio galaxy 3C 120 Gómez et al. (1998, 2000) found several components being associated with the ejection of a single major superluminal component. Furthermore, the passage of this new superluminal component ("O" in Fig. 3) triggered the appearance of a stationary feature ("M" in Fig. 3) that presents also enhanced linearly polarized emission. This behavior is in agreement with the numerical simulations of the trailing shocks by Agudo et al. (2001a).

VLBI observations of the superluminal microquasars GRO J1655-40 (Hjellming & Rupen 1995; Tingay et al. 1995) and GRS 1915+105 (Fender et al. 1999; Dhawan, Mirabel, & Rodríguez 2000) show a more complex jet structure than usually observed in jets of AGNs. The jets in GRO J1655-40 present alternate brightening and fading that cannot be interpreted in terms of relativistic beaming alone (Hjellming & Rupen 1995). These observations may be revealing some of the complex hydrodynamical process that are expected to manifest in high resolution images, such as interactions of the jet with the external medium (the jets in GRO J1655-40 are believed to be precessing with a period of three days). Similar complex components evolution have also been observed in 3C 120, interpreted as the interaction of the jet with a

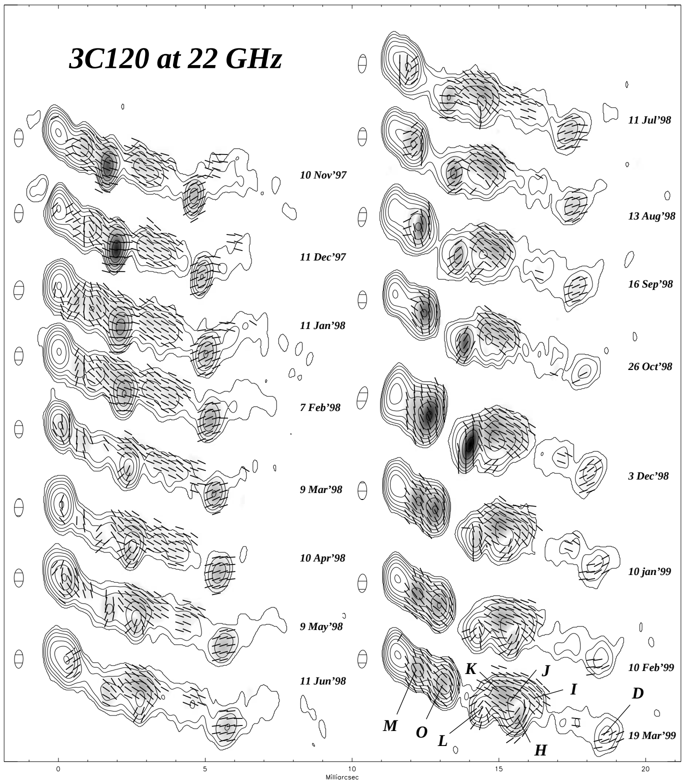

Figure 3. Monthly 22 GHz VLBA observations of the jet in the radio galaxy 3C 120 (from Gómez et al. 2000). Total intensity is plotted in contours, linearly polarized intensity in gray scale, and magnetic vectors with bars.

cloud of ionized gas located at about 8 pc from the center of the galaxy (Gómez et al. 2000).

4.0. Magnetic fields

Polarimetric observations of the jets in AGNs and microquasars is of special relevance. Determination of the magnetic field structure and strength is needed to obtain a better understanding of the superluminal components nature (shocks or blobs), as well as to test the models for jet formation and collimation.

The low fluxes exhibited by the jets in microquasars make polarimetric VLBI observations of these objects a very difficult task. One of the few observations corresponds to MERLIN observations of GRS 1915+105 (Fender et al. 1999). Linearly polarized emission was detected in the leading superluminal component of the approaching jet, revealing a changing polarization angle with time, accompanied by a depolarization. This is interpreted as evidence for a randomization of the magnetic field in the component. These observations contrast with the predictions of the shock-in-jet models, suggesting that components in GRS 1915+105 may instead consist of discrete plasmons.

Aloy et al. (2000) have studied the radio emission properties of 3D relativistic hydrodynamical jets. The interaction between the relativistic jet and the ambient medium results in a jet stratification where a fast spine is surrounded by a slow high energy shear layer. By introducing an ad-hoc helical magnetic field in the sheath, the authors found that the emission shows a cross section asymmetry, which is a function of the viewing angle and flow velocity. This may explain the otherwise puzzling asymmetric polarization structure observed in the blazar 1055+018 (Attridge, Roberts, & Wardle 1999).

5. Conclusions

Numerical relativistic (magneto)hydrodynamical and emission simulations have proven to be a powerful method to understand the physics of jets in AGNs and microquasars through a direct comparison with observations. Some perspectives for the future in numerical simulations would be: i) the exploration of different equations of state that would help to determine the jet composition (pairs or baryonic); ii) inclusion of radiative losses and particle acceleration (i.e., Jones, Ryu, & Engel 1999) as well as implementation of high energy emission mechanisms (inverse Compton) that would help to obtain a better understanding of the emission at high energies (X and γ rays); iii) study of the jet-external medium interactions, that seems to be more common than previously thought (i.e., Gómez et al. 2000); and iv) computation of the emission from relativistic magnetohydrodynamical models that would be of great help to understand the magnetic field influence in the jet dynamics, helping to explain recent and upcoming polarimetric VLBI observations.

Acknowledgements

This research is supported in part by the Spanish DGICT under grant PB97-1164.

References

Agudo, I., Gómez, J. L., Martí, J. M., Ibáñez, J. M., Marscher, A. P., Alberdi, A., Aloy, J. M., & Hardee, P. E. 2001a, ApJ, in press

Agudo, I., Gómez, J. L., Martí, J. M., Ibáñez, J. M., Marscher, A. P., Alberdi, A., Aloy, J. M., & Hardee, P. E. 2001b, These proceedings
Aloy, M. A., Ibáñez, J. M., Martí, J. M., & Müller, E. 1999a, ApJS, 122, 151
Aloy, M. A., Ibáñez, J. M., Martí, J. M., Gómez, J. L., & Müller, E. 1999b, ApJ, 523, L125
Aloy, M. A., Gómez, J. L., Ibáñez, J. M., Martí, J. M., & Müller, E. 2000, ApJ, 528, L85
Attridge, J. M., Roberts, D. H., & Wardle, J. F. C. 1999, ApJ, 518, L87
Dhawan, V., Mirabel, I. F., & Rodríguez, L. F. 2000, ApJ, 543, 373
Duncan, G. C., & Hughes, P. A. 1994, ApJ, 436, L119
Fender, R. P., Garrington, S. T., McKay, D. J., Muxlow, T. W. B., Pooley, G. G., Spencer, R. E., Stirling, A. M., & Waltman, E. B. 1999, MNRAS, 304, 865
Ferrari, A. 1998, ARA&A, 36, 539
Gómez, J. L., Martí, J. M., Marscher, A. P., Ibáñez, J. M., & Marcaide, J. M. 1995, ApJ, 449, L19
Gómez, J. L., Martí, J. M., Marscher, A. P., Ibáñez, J. M., & Alberdi, A. 1997, ApJ, 482, L33
Gómez, J. L., Marscher, A. P., Alberdi, A., Martí, J. M., & Ibáñez, J. M. 1998, ApJ, 499, 221
Gómez, J. L., Marscher, A. P., Alberdi, A., Jorstad, S. G., & García-Miró, C. 2000, Science, 289, 2317
Hardee, P. E. 2000, ApJ, 533, 176
Hjellming, R. M., & Rupen, M. P. 1995, Nature, 375, 464
Hughes, P. A., Aller, H. D., & Aller, M. F. 1985, ApJ, 298, 301
Hughes, P. A. 2000, in *Particles and Fields in Radio Galaxies*, ed. R. A. Laing & K. M. Blundell (ASP Conference Series Vol. 201). Available as astro-ph/0011127
Jones, T. W., Ryu, D., Engel, A. 1999, ApJ, 512, 105
Koide, S., Shibata, K., & Kudoh, T. 1999, ApJ, 522, 727
Komissarov, S. S., & Falle, S. A. E. G. 1997, MNRAS, 288, 833
Komissarov, S. S., & Falle, S. A. E. G. 1998, MNRAS, 297, 1087
Komissarov, S. S. 1999, MNRAS, 308, 1069
Marscher, A. P., & Gear, W. K. 1985, ApJ, 298, 114
Martí, J. M., Müller, E., & Ibáñez, J. M. 1994, A&A, 281, L9
Martí, J. M., Müller, E., Font, J. A., & Ibáñez, J. M. 1995, ApJ, 448, L105
Martí, J. M., Müller, E., Font, J. A., Ibáñez, J. M., & Marquina, A. 1997, ApJ, 479, 151
Martí, J. M., & Müller, E. 1999, Living Reviews in Relativity, http://www.livingreviews.org/Articles
Martí, J. M. 2000, in *AGNs in their Cosmical Environment*, eds. B. Rocca-Volmerange, & H. Sol, EDP Series in Astronomy and Astrophysics (EDP Sciences), en prensa
Meier, D. 2001, These proceedings
Mioduszewski, A. J., Hughes, P. A., & Duncan, G. C. 1997, ApJ, 476, 649
Mirabel, I. F., & Rodríguez, L. F. 1999, ARA&A, 37, 409
Norman, M. L. 1996, in *Energy Transport in Radio Galaxies and Quasars*, ed. P. E. Hardee, A. H. Bridle & J. A. Zensus (ASP Conference Series, Vol. 100), p. 405
Rodríguez, L. F. & Mirabel, I. F. 1999, A&A, 340, L47
Rosen, A., Hughes, P. A., Duncan, G. C., & Hardee, P. E. 1999, ApJ, 516, 729
Tingay, S. J. et al. 1995, Nature, 374, 141
van Putten, M. H. P. M. 1993, ApJ, 408, L21

Jets in XRB Low/Hard States: Models of XTE J1118+480 suggest a strong signature from radio through X-ray *

S. Markoff† and H. Falcke
Max-Planck-Institut für Radioastronomie, Bonn, Germany

R. Fender
Astronomical Institute "Anton Pannekoek", University of Amsterdam, Netherlands

Keywords: X-ray binary, jet, black hole physics, radiation mechanisms:non-thermal

Summary

Observations reveal the presence of powerful jets in the Low/Hard states of several black hole candidate X-ray binaries, so it is important to consider what signatures these outflows will have in the broadband Low/Hard spectrum. Correlations between the radio and X-rays, as well as in at least one case the optical, suggest that emission from a jet, via either synchrotron or inverse Compton (IC) processes, may play a role. The recently discovered X-ray transient XTE J1118+480 (Remillard et al. 2000), a black hole candidate in the Low/Hard X-ray state, provides an excellent opportunity for multi-wavelength modeling, since it has been observed not only in the radio through X-rays (see Fender et al. 2000, and references therein), but is also at high enough Galactic latitude to allow the first ever EUV detections of an X-ray transient (Hynes at al. 2000, hereafter H00).

We consider a simplistic scenario of symmetric, magnetized relativistic plasma outflows. The jet plasma encounters a shock, which accelerates the particle distribution into a power-law, creating a jump in the spectrum where the shock-accelerated leptons produce an optically thin power-law extending to the X-ray regime. The details of this calculation, as well as a more evolved model which addresses the presence of an accretion disk component, can be found in Falcke & Markoff (2000), Markoff, Falcke & Fender (2000), respectively, and references therein. We include a representative figure, which includes only synchrotron emission from the jet. Surprisingly, we can account for the radio-IR and the X-ray data reasonably well without invoking an IC component or the presence of significant disk emission.

* We are grateful to the (late) Bob Hjellming for sharing his data with us.
† Supported by a Humboldt Research Fellowship

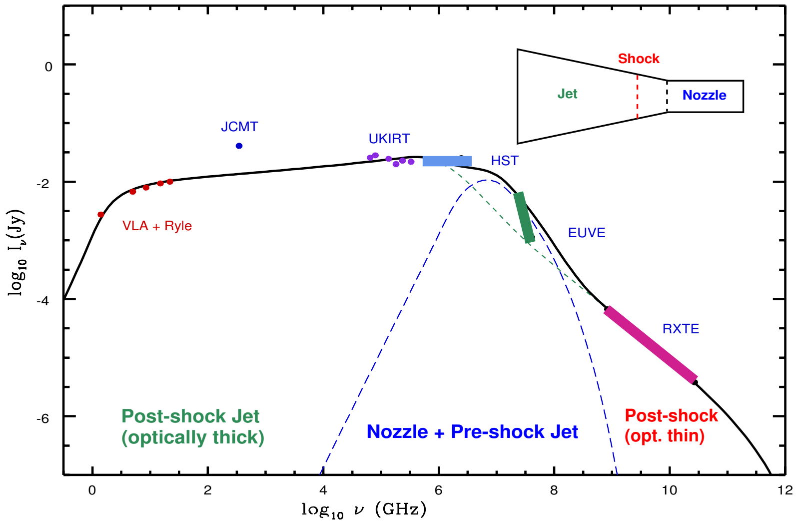

Figure 1. Fit for power-law spectral index 2.6, $M_{\rm bh} = 5M_{\odot}$, $L = 0.04L_{\rm Edd}$, $z_{\rm sh} = 16r_s$, and inclination angle 40°. Data points from H00 except radio (Hjellming et al., in prep.), and JCMT (Fender et al. 2000). We cannot account for the entire optical range from the jet alone, but the detection of strong H_α lines (Garcia et al. 2000) could be indicative of disk emission at these frequencies. We use the maximum absorption case presented in H00 for the EUVE data. Included is a schematic explaining the different emission regions. The JCMT point obviously is well outside the range of this model, which could be accounted for either by the addition of another shock further out, resulting in enhanced emission, or by thermal emission from a torus.

As an interesting note, the hard X-rays have been seen lagging the soft in several XRBs (e.g., Ford et al. 2000). A multi-component model such as that presented here, or including disk emission (see Markoff et al. 2000) is favorable.

References

Falcke, H. & Markoff, S., 2000, A&A, in press
Fender, R.P., Hjellming, R.M., Tilanus, R.J., Pooley, G.G., Deane, J.R., Ogley, R.N., Spencer, R.E., 2000, MNRAS, submitted
Ford, E.C., van der Klis, M., Méndez, M., Wijnands, R., Homan, J., Jonker, P.G., van Paradijs, J., 2000, ApJ, 537, 368
Garcia, M., Brown, W., Pahre, M., McClintock, J., Callanan, P., Garnavich, P., 2000, IAU Circ. 7392
Hynes, R.I., Mauche, C.W., Haswell, C.A., Shrader, C.R., Cui, W., Chaty, S., 2000, ApJL, 539, L37
Markoff, S., Falcke, H., Fender, R., 2000, ApJL, submitted
Remillard, R., Morgen, E., Smith, D., Smith, E., 2000, IAU Circ. 7389

The disc – jet connection in GRS 1915+105

Klein-Wolt, M.[1], Fender, R.P.[1], Pooley, G. G.[2], Belloni, T.[3], Migliari, S.[3,4], Morgan, E. H.[5], van der Klis, M.[1]
[1]*API Amsterdam,* [2]*MRAO Cambridge,* [3]*OAB Merate,* [4]*Univ. Milano,* [5]*MIT Cambridge*

Abstract. We present an analysis of simultaneous X-ray and radio observations of the black hole candidate GRS 1915+105.

1. Introduction

The black hole candidate GRS 1915+105 is known for its extremely complex X-ray behaviour, which is not observed in any other X-ray source. Belloni et al. (2000) succesfully described this behaviour as transitions between three basic spectral states: the soft states A and B, and the hard state C. GRS 1915+105 was discovered in 1994 to be the first galactic source to show superluminal motions of radio-emitting ejecta (Mirabel & Rodriguez 1994). Besides these big radio flares, the source also shows smaller radio oscillation events with periods around 20-40 minutes (Pooley & Fender 1997).

2. Comparing the simultaneous radio and the X-ray observations

We have cross-correlated simultaneous (15 GHz) Ryle Telescope (RT) radio and Rossi X-Ray Timing Explorer (RXTE; PCA, 2-60 KeV) X-ray observations of GRS 1915+105 made between June 12, 1996 and December 13, 1999, to find a total of 105 overlapping observations (about 9170 minutes of data). In Fig. 2 we show one representative observation. The X-ray light curve (lower panel) is broken up into states A, B, C. From spectral fits (see Migliari, Vignarca & Belloni (this volume)) it can be concluded that during the spectrally hard state-C dips the inner part of the accretion disc is either missing or just unobservable. The radio emission, at the same time, shows an oscillating flaring type of behaviour for which the period is found to be between 20 and 40 minutes. We also found observations which do not have state C intervals and consist of state A and B alone. For these observations the inner radius of the accretion disc does not change much and importantly, the radio emission is strongly suppressed: the flux density is typically less than a few mJy, despite up to 50% variability in the X-ray flux.

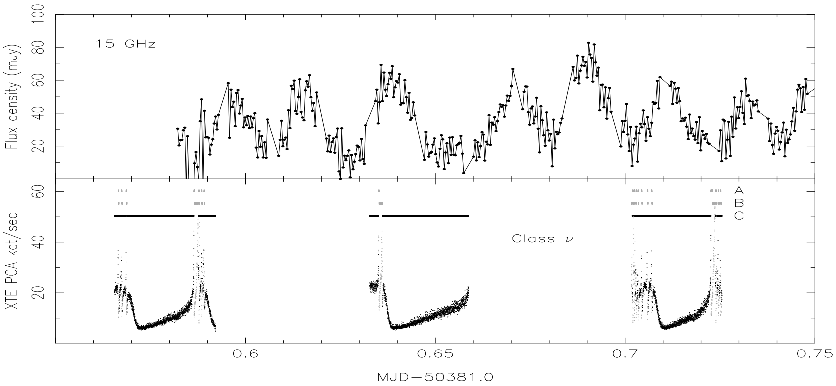

Figure 2. Overlapping Radio/X-ray observation showing the hard X-ray dips (state C), and the radio oscillation events. The rms noise is 3 mJy per point in the radio.

We find that radio oscillations require the presence of long ($\geq$100s) state C intervals; for observations consisting of state A and B only the radio emission is suppressed (typically less than a few mJy). With short state C intervals less than 100s in length only very weak radio emission ($\sim$5 mJy) is observed. The long state-C intervals correspond to *hard* dips in the X-ray light curve which seem to have a one-to-one relation with the radio events: each hard dip produces a new radio "flare".

During long "plateau" states, when the source is believed to be in state C for up to weeks at a time, a (large) quasi-continuous jet is formed with an almost flat synchrotron spectrum extending to at least the near-infrared. We suggest that both for these large jets and the radio oscillation events shown in Fig. 2 the same mechanism could be responsible for the production of the radio emission: during a state C interval the corona and the jet are coupled (or are the same structure) and an outflow takes place. As the material moves downstream in the jet, it becomes optically thin at progressively lower frequencies. This causes the observed delay between the radio and the X-ray emission. The plateau states are just longer and more stable versions of the state C intervals: continuous ejection causes a superposition of optically thick and thin parts to be observed as spectrally flat.

References

Belloni T., Klein-Wolt M. et al., 2000, A&A, 355, 271
Mirabel I.F., Rodríguez L.F., 1994, Nature, 371, 46
Pooley G.G., Fender R.P., 1997, MNRAS, 292, 925

Hydrodynamical and Emission Simulations of Relativistic Jets: Stability and Generation of Superluminal and Stationary Components

Iván Agudo and José-Luis Gómez
Instituto de Astrofísica de Andalucía, CSIC, Granada, Spain

José-María Martí and José-María Ibáñez
Departamento de Astronomía y Astrofísica, Universidad de Valencia, Valencia, Spain

Alan P. Marscher
Institute for Astrophysical Research, Boston University, Boston, USA

Antonio Alberdi
Instituto de Astrofísica de Andalucía, CSIC, Granada, Spain

Miguel-Ángel Aloy
Max-Planck-Institut für Astrophysik, Garching, Germany

Philip E. Hardee
Department of Physics and Astronomy, University of Alabama, Tuscaloosa, USA

Abstract. We present 2D hydrodynamical and emission simulations of the jet stability after the introduction of strong perturbations on a relativistic jet. These simulations show that the interaction of a *single* strong perturbation with the underlying jet results in the formation of multiple conical shocks with very specific observational properties.

Keywords: jet, hydrodynamics, radiation mechanisms:non-thermal, general relativity.

1. The jet model

Stationary and superluminal components are commonly observed in jets of AGNs and microquasars, usually associated with stationary and moving shocks. Here we describe a general mechanism for the generation of superluminal and stationary components in relativistic jets. We have used a 2D hydrodynamical code (see Martí et al., 1997 and references therein) to compute the time evolution of a relativistic jet after the introduction of a strong square-wave perturbation at the jet inlet. Our steady jet model consists of a supersonic relativistically ideal gas in pressure equilibrium with a denser external medium and with a Lorentz factor of 4 at the jet inlet. The jet has an opening angle of 0.3° induced by a decreasing pressure gradient in the external medium. The square-wave perturbation in the steady jet model consists in an increase of the inlet Lorentz factor and pressure during a short time interval (for more details see Agudo et al., 2000). The hydrodynamical results are used to compute the synchrotron radio emission (see Gómez et al., 1997 and references therein), at a viewing angle of 10°, considering all the relativistic effects, including the time delays.

2. Results

Our simulations show that the passage of a strong perturbation through a jet triggers a local pinch instability (Hardee, 2000 and references therein) in the surface of the jet, leading to the formation of a series of conical *trailing shocks*. The analysis of the emission simulations in time predicts very specific observational properties for these features (Agudo et al., 2000). The *trailing components*, as we call the counterpart of the trailing shocks in the emission simulations, appear upstream of the superluminal component associated with the perturbation induced at the jet inlet. Therefore, trailing components can be easily *observationally* distinguished from those generated at the jet inlet (which could be associated with the VLBI core): they would emanate not from the core, but rather would seem to appear spontaneously downstream, created in the wake of strong perturbations. Those components appearing close to the core are very stable both in position and flux densities and therefore may be associated with stationary components, in contrast to components appearing further downstream that show larger apparent motions (episodically superluminal, but always with lower velocities than the main superluminal component) as well as weaker flux densities. They are related to conical shocks, and hence should exhibit different polarization properties from those of the main component. VLBI observations can provide dynamic ranges of the order of 200:1 or larger. All components seen in our simulated radio maps are above this limit, and therefore are expected to be detected by actual VLBI arrays. Our simulations support the idea that jets can be steadier than previously thought, because multiple components in radio maps can be produced by a single ejection event.

References

Agudo, I., Gómez, J. L., , Martí, J. M. et al.: 2000, *ApJ Letters*, in press
Gómez, J. L., Martí, J. M., Marscher, P. A. et al.: 1997, *ApJ*, **482**, L33–L36
Hardee, P. E.: 2000, *ApJ*, **533**, 176–193
Martí, J. M., Müller, E., Font, J. A. et al.: 1997, *ApJ*, **479**, 151–163

Magnetorotational ejection.

N.V. Ardeljan (ardel@redsun.cs.msu.su)
Department of Computational Mathematics and Cybernetics, Moscow State University, Vorobjevy Gory, Moscow B-234 119899, Russia

G.S. Bisnovatyi-Kogan (gkogan@mx.iki.rssi.ru)
Space Research Institute, Profsoyuznaya str. 84/32, Moscow 117810, Russia

S.G. Moiseenko (moiseenko@mx.iki.rssi.ru)
Space Research Institute, Profsoyuznaya str. 84/32, Moscow 117810, Russia

Abstract. We consider the ejection of matter produced by amplification of the toroidal component of the magnetic field due to differential rotation in a star. Part of the rotational energy is transformed into kinetic energy of radial motion. About 7% of the mass of the star acquires kinetic energy larger than its potential energy and can be ejected. 2D simulations have been performed using a specially-developed implicit Lagrangian method on a triangular grid with mesh restructuring.

Keywords: MHD, ejection, collapse

We have performed 2D simulations of the magnetorotational ejection mechanism, suggested by Bisnovatyi-Kogan(1970). Amplification of the toroidal component of the magnetic field due to differential rotation leads to the transformation of a part of the rotational energy to kinetic energy of ejection. The first numerical simulations devoted to the magnetorotational mechanism were made by Le Blanc and Wilson (1970) and investigated analytically in the paper by Meier et.al. (1976).

One of the most important parameters for this problem is the ratio of magnetic energy to gravitational energy in the star: $\alpha = \frac{E_{\rm mag}}{|E_{\rm grav}|}$. We have performed simulations for initial values of $\alpha = 10^{-2}$, $10^{-4}, 10^{-6}$. The initial magnetic field for the problem should satisfy the following requirements: 1.it should be divergence-free; 2.it should be balanced (i.e. the force produced by the magnetic field should be in balance with other forces in the star); 3.it should be stable. Details of the definition of the initial magnetic field are described in the paper by Ardeljan et al. (2000).

For the simulations we used a specially-developed Lagrangian 2D numerical implicit scheme on a triangular grid with mesh reconstruction (see Ardeljan and Kosmachevskii., 1995 and references therein).

The initial magnetic field chosen for our simulations has quadrupole-like symmetry (i.e. its "z"- component is equal to zero at the equatorial plane). This is why we obtain radial ejection (Fig.1), instead of a jet. Application of an initial magnetic field with dipole-like symmetry should produce a jet, as in Le Blanc and Wilson (1970).

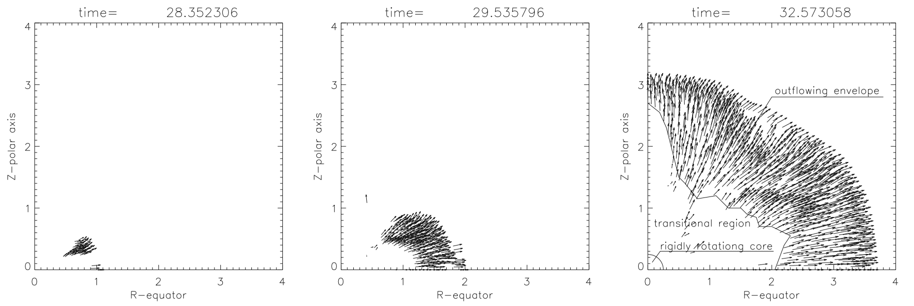

Figure 1. Ejected part of the envelope of the star at $t = 28.352$ (*left*), $t = 29.536$ (*center*) and at $t = 32.573$ (*right*).

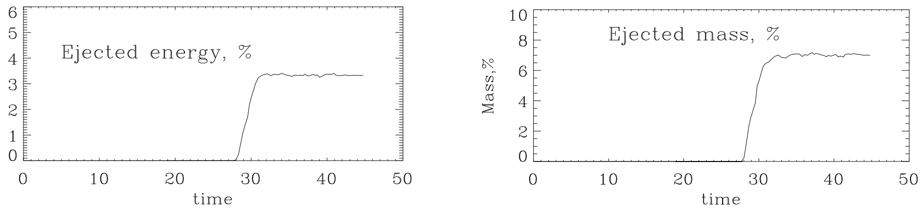

Figure 2. Left figure: Time evolution (in % to the total initial energy of the cloud) of the energy of the ejected matter of the envelope of the star. *Right figure*: Time evolution (in %) of the ejected mass of the envelope of the star.

The toroidal magnetic field grows with time and produces an MHD shock, which moves to the boundary of the star.

Part of the matter of the envelope of the star (about 7% of the mass of the star) has radial kinetic energy larger than its potential energy and can be ejected. This ejected matter carries about 3.3% of the total energy of the star. Fig.2 presents the time evolution of the ejected mass and energy.

Acknowledgements G.S.B.-K. and S.G.M. thank Dr. A.Castro-Tirado for hospitality, RFBR for partial support by grants 98-01-00352, 99-02-18180 and ESA-INTAS grant No.120.

References

Ardeljan, N. V., Bisnovatyi-Kogan, G. S., Moiseenko, S. G. *A&A*, **355**, 1181-1190, 2000.

Ardeljan, N. V., Kosmachevskii, K. V. *Computational and Mathematical Modeling*, 6: 209-224, 1995.

Bisnovatyi-Kogan, G. S. *Astron. Zh.*, 47: 813-816, 1970.

Le Blanc, L. M., Wilson, J. R. *ApJ*, 161: 541-551, 1970.

Meier, D. L., Epstein, R.I., Arnett, W.D., Schramm, D.,N. *ApJ*, 204: 869-878, 1976.

Stationary relativistic magnetic jets from black holes

Christian Fendt and Elisabetta Memola
Astrophysikalisches Institut, An der Sternwarte 16, 14482 Potsdam, Germany

Abstract. We investigate the jet formation region of relativistic magnetic jets using stationary axisymmetric MHD models. We numerically calculate the field structure of the collimating jet and the flow acceleration. Special or general relativistic effects are considered. Stationarity allows for a *global* treatment of the jet physics. Our results are applicable to highly relativistic jets of AGN and microquasars.

Keywords: magnetic jets, microquasar

1. Stationary relativistic MHD

The stationary and axisymmetric ideal MHD equations can be reduced to the Grad-Shafranov equation (GSE) and the wind equation, describing the force-balance across and along the flux surfaces $\Psi \sim \int \vec{B}_P \cdot d\vec{A}$. The GSE is a non linear partial differential equation of second order for Ψ with the source term depending on the total poloidal current $I(\Psi)$ and the iso-rotation parameter $\Omega_{\rm F}(\Psi)$ [cf.1,4,5]. At the light surface of the magnetosphere the GSE becomes singular. The stationary polytropic wind equation can be converted in a polynomial equation for the poloidal velocity $u_{\rm p} \equiv \gamma v_{\rm p}/c$ [2,3,6,7].

2. Two-dimensional structure of the magnetic jet

Our example solutions of the special relativistic GSE with constant $\Omega_{\rm F}$ were calculated with increasing strength of the poloidal electric current demonstrating its collimating effect. We show meridional cuts across the axisymmetric magnetic flux surfaces (Fig. 1, *left*). The outer boundary is the light cylinder imposing the regularity condition.

Global magnetic jets calculated from the GSE in Kerr metric were presented in [4]. In general, the asymptotic jet radius is several light cylinder radii. To consider differentially rotating field line foot points is an essential step since jets are anchored in differentially rotating disks [5]. As a consequence, the shape of the light surface is not known a priori and must be calculated iteratively together with the GSE solution. The global field is then determined by a smooth transition of the field across the light surface (Fig. 1, *right*). Differential rotation, $\Omega_{\rm F}(\Psi)$, leads to stronger collimation.

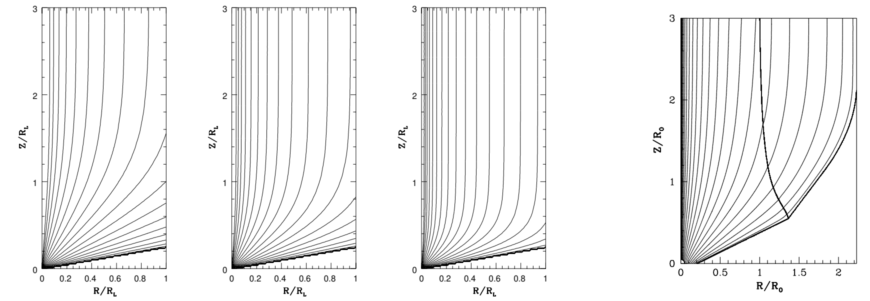

Figure 1. Jet magnetic flux distribution $\Psi(R,Z)$. Radius in units of light cylinder radii R_L or asymptotic light surface radii R_0. *Left*: influence of electric current (increasing by factors of 1,2,5 from left). *Right*: differentially rotating foot points.

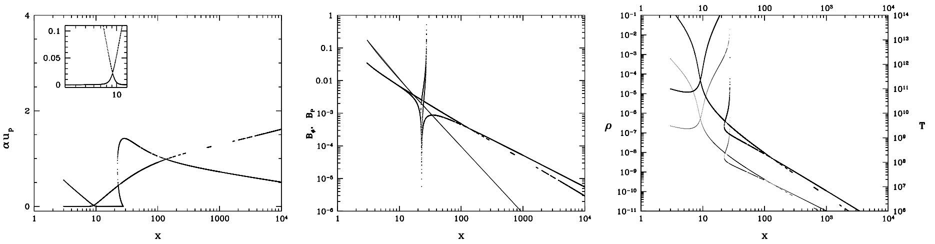

Figure 2. The two branches of the magnetic wind solution in Kerr metric ($a = 0.8$). Poloidal 4-velocity u_P and the corresponding branches of magnetic field B_p, B_ϕ, temperature T and density ρ . The jet solution is the branch with increasing velocity. Intersections indicate the 3 magnetosonic points. Radius x in units of the horizon.

3. Magnetic jet acceleration in Kerr metric

Solutions of the wind equation in Kerr metric prove that a relativistic jet speed $> 0.9\,c$ can be achieved for microquasars (Fig.2) [7]. The field strength at the jet origin is 10^9G. At large radii the field is toroidally dominated. A highly magnetized jet flow becomes highly relativistic, even if its origin is *not* close to the horizon ($x \sim 10$). Temperature and density decrease logarithmically (from 10^{10}K to 10^6 at a distance of ~ 1000). X- and γ-emission should be detected from the inner jet.

References

[1] Okamoto I., 1992, MNRAS, 254, 192
[2] Camenzind M., 1986, A&A, 162, 32
[3] Takahashi M., Nitta S., Tatematsu Y., Tomimatsu A., 1990, ApJ, 363, 206
[4] Fendt Ch, 1997, A&A, 323, 999
[5] Fendt Ch, Memola E. 2001, A&A, in press
[6] Fendt Ch., Camenzind M., 1996, A&A, 313, 591
[7] Fendt Ch., Greiner J., 2001, A&A, in press

Positron-electron Annihilation Line of Relativistic Jet in AGNs and Quasars *

Jian-Min Wang[1], Ph. Durouchoux[2] and Ti-Pei Li[1]
1. Laboratory of Cosmic Ray and High Energy Astrophysics, IHEP, Beijing 100039, China
2. CE Saclay, DSM, DAPNIA, Service d'Astrophysique, 91191 Gif sur Yvette Cedex, France

Abstract. We pointed there are two possible regions producing positron-electron annihilation line (PEAL) from the relativistic jet: close to and far away from the black hole in AGNs and quasars. The PEAL profile has been calculated for several cases. It is expected that future observations with *INTEGRAL* may discover these lines in order to test the paradigm of active galactic nuclei and quasars.

1. Introduction

It has been generally realized that there is a copious $e^{\pm}$ plasma in active galactic nuclei and quasars. Recently Wang (2000) argue that the interaction between the very high energy (VHE) photons and the synchrotron photons reflected by clouds in broad line region may produce a large electron-positron cloud. Such a cloud is moving with relativistic velocity. Therefore the observed PEAL is simply Doppler shifted towards to the blue for small viewing angle. The second source of producing PEAL is that $e^{\pm}$ blob may be ejected from the nucleus with highly relativistic speed (Li & Liang 1996, Beloborodov 1999, Spruit 2000, Wang et al. 2000a). PEAL from such a moving blob close to a rotating black hole may be seriously distorted by gravitational effects. Wang et al. (2000b) calculate the PEAL profiles from such a blob. In general the profiles are characterized by two peaks.

2. Profile of Positron-electron Annihilation Line

2.0. Inner Region of Jet

PEAL profile should be affected by both speciall and general relativistic effects. The profiles from approaching jet are different from that from receding jet. The detail profiles received by an observer at infinity with different viewing angles can be found in Wang et al. (2000b).

* send offprint requests to: Jian-Min Wang *wangjm@astrosv1.ihep.ac.cn*

2.0. Outer Region of Jet

Although the deficiency of very high energy emission from γ-loud blazars may be due to the absorption of cosmological background radiation, Wang (2000) argue that there is an *intrinsic* mechanism responsible for the absorption of VHE photons by the reflected synchrotron (RSy) photons. We argue that the energy density of the RSy photons is higher than that of the local synchrotron photons. The VHE emission is thus constrained by RSy photons. The opacity of the pair production due to photon interaction can be expressed by the observable quantities

$$\tau_{\gamma\gamma}(\epsilon_{\rm obs}) = 2.0\, l_{\rm rsc}^{-1}\mathcal{D}_{10}^{4}\left(\frac{\epsilon_{\rm obs}}{\rm TeV}\right)^{0.7}\left(\frac{\Delta t_{\rm obs}}{\rm day}\right)\left(\frac{\nu_{\rm s}}{4.0\times 10^{3.7}}\right)^{3.7}\left(\frac{\nu_{\rm rsc}}{10^{25}{\rm Hz}}\right)^{-2} \tag{1}$$

where Doppler factor $\mathcal{D}_{10}=\mathcal{D}/10$, $\Delta t_{\rm obs}$ is the timescale of the variation of γ-ray, $\nu_{\rm s}$ and $\nu_{\rm rsc}$ are the peak frequency at low and high energy bands, respectively. This formula is available for electron spectral index $\alpha = 2.4$. It should be addressed here is the parameter $l_{\rm rsc}$, representing the ratio of the peak flux at high energy (γ) band to that at low energy band. The larger $l_{\rm rsc}$ the larger pair opacity is, namely, there is a larger $e^{\pm}$ cloud in quasars.

If the deficiency of VHE from γ-ray loud blazars is indeed due to this *intrinsic* mechanism, it is expected that future observation should discover the PEAL at $5\mathcal{D}_{10}$MeV. Its profile is rather simple since onely Doppler effect works in such an outer region.

3. Conclusions

We should choose the high $l_{\rm rsc}$ blazars as the observable objects in future observations. The complex profiles of an emission line depends on the viewing angle. It is expected that future observations with *INTEGRAL* may discover the complex PEALs.

References

Beloborodov, A, 1999, MNRAS, 305, 181
Li, H., & Liang, E., 1996, ApJ, 458, 514
Spruit, H.C., 2000, astro-ph/0003043
Wang, J.-M., 2000, ApJ, 538, 181
Wang, J.-M., Yuan, Y.-F., Wu, M. & Kusunose, M., 2000a, ApJ, 541, L41
Wang, J.-M., Zhou, Y.-Y., Yuan, Y.-F, & Cao, X., 2000b, ApJ, 544, in press (astro-ph/0006268)